AUTOMATED MANUFACTURING OF ORTHODONTIC APPLIANCES

By

Scott Cameron Roberts

B.A.Sc. (Mechanical Engineering) University of British Columbia

A THESIS SUBMITTED IN PARTIAL FULFILLMENT OF

THE REQUIREMENTS FOR THE DEGREE OF

MASTER OF APPLIED SCIENCE

in

THE FACULTY OF GRADUATE STUDIES

MECHANICAL ENGINEERING

We accept this thesis as conforming

to the required standard

THE UNIVERSITY OF BRITISH COLUMBIA

June 1991

In presenting this thesis in partial fulfilment of the requirements for an advanced degree at the University of British Columbia, I agree that the Library shall make it freely available for reference and study. I further agree that permission for extensive copying of this thesis for scholarly purposes may be granted by the head of my department or by his or her representatives. It is understood that copying or publication of this thesis for financial gain shall not be allowed without my written permission.

Department of Mechanical Engineering

The University of British Columbia
Vancouver, Canada

Date 12 June 1991

DE-6 (2/88)

Abstract

This thesis presents a computer controlled system that partially automates the production of upper-mouth orthodontic appliances. The machine performs the deposition and curing required to manufacture the acrylic portion of the appliance. Under this new process, the operator places the orthodontic wires and expansion screws on the surface of the dental cast, secures the cast onto the machine and describes the desired shape of the appliance through a graphical user interface. The machine then applies and cures the acrylic to form the finished appliance. Only minimal grinding and buffing is required.

The system consists of a robotic device that includes a two-axis platform for manipulating dental casts; and a two-axis gantry for positioning an acrylic pump, ultraviolet lamp, laser and rotating mirror system, and a camera. The laser and camera are part of a range vision system for mapping the surface of the dental cast to obtain elevation and surface normal data. The pump and lamp are used to deposit and cure light activated liquid acrylic. The rotary table system provides orientation for the dental cast to permit surface mapping and acrylic deposition and curing. The table is able to orient the dental cast to avoid movement of the liquid acrylic on the surface of the cast before curing takes place. The machine software provides tool-workpiece collision avoidance, process planning, and machine function and motion control.

Several tests, including the complete production of orthodontic appliances, have been performed with the system. The average time for surface mapping of a dental cast is 11.5 minutes and the average time for acrylic deposition and curing is 54.3 minutes.

Table of Contents

Abstract ii

List of Figures vii

List of Tables viii

Nomenclature ix

Acknowledgement xii

1 Introduction 1

2 Process Overview 5

2.1 Orthodontics 5

2.2 Current Methods of Manufacture 7

2.3 Computer Vision Surface Measurement Techniques 9

3 Machine and Process Description 15

3.1 Functional Specification 15

3.1.1 Task Description 15

3.1.2 Process Description 17

3.2 Machine Description 20

3.2.1 Dental Cast Manipulation 21

3.2.2 Dental Cast Surface Mapping 21

3.2.3 Acrylic Deposition and Curing 23

3.2.4 Machine Configuration 23
3.2.5 Electronics and Control 27

4 System Operation **31**
4.1 Kinematics 31
4.1.1 Coordinate Frames 31
4.1.2 Transformation of a Point Between Frames 32
4.1.3 Forward Kinematics 35
4.2 Inverse Kinematics 38
4.2.1 Determination of θ_r and θ_t 39
4.2.2 Determination of L_3 and L_5 41
4.3 Dental Cast Surface Mapping 42
4.3.1 Overview 42
4.3.2 Image Processing 43
4.3.3 Data Transformation and Storage 47
4.3.4 Surface Normal Calculation 51
4.4 Trajectory Planning and Generation 53
4.4.1 Path Planning 53
4.4.2 Collision Avoidance 55

5 Experimental Results **60**
5.1 Machine Construction 60
5.2 Appliances 60
5.3 Acrylic Pump and Curing Lamp 64
5.4 Image Processing 66
5.5 Motion Control 66
5.6 Future Work 67

6 Conclusions and Recommendations 69

Bibliography 71

Appendices 76

A Process Times 76

B Surface and In-Plane Normal Comparison 79

C Image Processing Analysis 81

D Machine Kinematic Parameters 83

E Control Loop Parameters 84

F Dental Cast Mapping Parameters 85

G Process Flow Charts 86

List of Figures

2.1 Typical removable orthodontic appliance 6

2.2 Dental cast made from rubber impression of mouth 8

3.1 Two axis rotary table system for dental cast manipulation 22

3.2 Active laser triangulation surface measurement 24

3.3 Machine components 25

3.4 Machine with coordinate frames and dimensions 26

3.5 Electrical and control flow diagram 28

3.6 D.C. motor control loop 30

4.1 Determining the in plane normal $\vec{N}$ 39

4.2 Determining the rotation θ_r 40

4.3 Pixel intensity for one column 44

4.4 Data processed with derivative operator 45

4.5 Midpoint accuracy versus scan section width 47

4.6 Basic cast dimensions 49

4.7 Cast outline superimposed on grid map 54

4.8 Encapsulating the table and cast with an ellipsoid 55

4.9 Collision avoidance 58

5.1 Experimental apparatus 61

5.2 Dental cast with wires and expansion screw 62

5.3 Finished appliance with wires and expansion screw 63

C.1 Number of cells scanned versus scan width 82

C.2 Number of cells replaced versus scan width 82

G.1 Process overview flowchart 86

G.2 Acrylic deposition and curing flowchart 87

G.3 Dental cast surface mapping flowchart 88

List of Tables

4.1 Denavit-Hartenburg parameters 36

4.2 Scan width database categories and representation 52

A.1 Cast dimensions 76

A.2 Scanning times 77

A.3 Acrylic deposition and curing times 77

A.4 Total process time 78

A.5 Resolution of stored data 78

B.1 In-plane normal orientation data 79

C.1 Image processing parameters 81

D.1 Machine parameters 83

E.1 Control loop parameters 84

F.1 Dental cast mapping parameters 85

Nomenclature

α:	Angle from X_t to gantry workspace
α_i:	Denavit-Hartenburg frame angle parameter
β:	Angle between $\vec{N}$ and $\vec{u}$
γ:	Angle between $\vec{N}$ and $\vec{v}$
ν:	Optical frequency of laser
θ_i:	Denavit-Hartenburg frame angle parameter
θ_r:	Rotational frame link position
θ_t:	Table frame link position
a:	Ellipse shape parameter (width)
a_i:	Denavit-Hartenburg frame length parameter
b:	Ellipse shape parameter (height)
C_{bc}:	Distance from base of dental cast to centre of table
C_{len}	Dental cast length
C_{wid}	Dental cast width
C_{yoff}:	CCD array centre pixel offset from workspace
C_{zb}:	Elevation at rear of dental cast
C_{zmax}:	Dental cast maximum elevation
C_{zmin}:	Dental cast minimum elevation
c:	Speed of light
d_i:	Denavit-Hartenburg frame distance parameter
f:	Frequency
f_b:	Beat frequency

f_m:	Modulation frequency
I:	Intensity
L_1:	Machine length parameter #1
L_2:	Machine length parameter #2
L_3:	Machine horizontal axis position parameter
L_4:	Machine length parameter #4
L_5:	Machine vertical axis position parameter
L_6:	Machine length parameter #6
L_7:	Machine length parameter #7
N:	Number of point to point moves
$\vec{N}$:	In-plane surface normal
N_{grid}:	Grid array side length
N_{mxy}:	Range map array size
N_{mz}:	Number of discrete range map elevations
N_p:	Pixel array size of CCD array
n:	Current point to point move
m:	Slope of a line
$\vec{n}$:	Surface normal
p:	Plane elevation operator
r:	Range operator
S:	Measure of slope for image processing
S_c:	Camera pixel calibration factor
S_{mxy}:	Range map spatial scale
S_{mz}:	Range map elevation scale
STD:	Standard Deviation

${}^{i}P_j$:	Position vector of a point j in frame i
${}^{i}_{j}R$:	Rotation matrix from frame j to frame i
${}^{i}_{j}T$:	Transformation from frame j to frame i
$\vec{u}$:	Vector in workspace of gantry in plane $Z_t = 0$
$\vec{v}$:	Vector in workspace of gantry along Z_t axis
W:	Distance from image plane to centre of lens
W_i:	Image processing width categories
Z:	Distance from object to centre of lens
Z_{coff}:	Pump nozzle offset for acrylic deposition

Acknowledgement

I would like to thank Dr. Farrokh Sassani of the Department of Mechanical Engineering for his guidance throughout this project. I would also like to thank Orthoflex Dental Laboratories for their invaluable technical support and donation of supplies. I am also indebted to Philip Pottier for his help with the system electronics and to Len Drakes for his work on the machine apparatus. This research was funded by a grant from the British Columbia Science Council.

This thesis is dedicated to Alex, in recognition of her patience and unfailing support throughout this work.

Chapter 1

Introduction

Today, orthodontic appliances are used by millions of children and young adults. With greater attention being paid to dental health care, the number and variety of orthodontic devices is increasing rapidly. This thesis presents a system that has been developed to partially automate the manufacture of orthodontic appliances.

High-Technology in Dentistry and Orthodontics

Computer methods and automated manufacture are slowly making an impact in the fields of dentistry and orthodontics. The transfer of new technology to an old market is stimulating the industry [1]. For example, the production of crowns has been revolutionized with the use of CAD/CAM and computer vision techniques. Rather than making a mould and then using conventional casting techniques, a computer vision system is used in the mouth to determine the correct shape and the crown is milled out of a ceramic block. This procedure results is improved quality and much faster production [2,3,4]. A patient can now be fitted with a crown in one sitting because of the improved production rate. Similar systems have been made for ceramic fillings and dental restorations. The possibility of using lasers as surgical scalpels in soft tissue operations and for fusing the enamel in root canals is also being investigated [5]. Finally, imaging systems are being used by dentists to show patients before and after treatment views of their teeth before work even begins. These new methods will benefit patients, manufacturers and dentists alike [1].

Orthodontics

Despite these recent technological advances, the method of preparation of orthodontic appliances has not changed significantly in 70 years - the most important mechanical therapies in orthodontics originated in the late 1920s and early 1930s [6]. Currently, appliances are prepared by making a plaster cast of a patient's mouth and teeth, bending and positioning retaining wires on the cast, and then manually depositing acrylic compounds in layers of liquid and powder to form an acrylic base.

The acrylic base fits the contours of the cast, secures the retaining wires, and houses adjustable expansion screws that apply corrective forces to the teeth via the wires and acrylic base itself. The appliance is trimmed with hand tools to the minimum size that holds the wires in position and which interferes least with the patient's breathing, swallowing and tongue movements while still having structural integrity. It is then polished with a grinding wheel to a smooth finish that is comfortable for the patient and prevents abrasion. The comfort of an appliance depends on the quality of its fit in the patient's mouth, a function of the skill and time spent by a technician in a labour intensive task.

Automated System for Acrylic Application

The system presented in this thesis automates the production of the acrylic portion of orthodontic appliances. The system incorporates machine vision, robotic manipulators (a computer controlled platform and gantry), process planning and collision avoidance software. The machine vision system, consisting of a laser, rotating mirror, CCD (charge coupled device) camera, and frame grabber, is used to map the surface of the dental cast to generate a three-dimensional computer model. The acrylic deposition and curing system, incorporating a pump and ultraviolet lamp, is used to apply and cure acrylic on the surface of the dental cast.

Three-dimensional mapping of the dental cast is performed by projecting a thin plane of laser light on the dental cast and analyzing the incident light with a computer vision system. Through an iterative process of changing the orientation of the cast and the elevation of the laser line, a full surface model of the cast is acquired. Elevation data from the three-dimensional surface model are used to determine the pump and lamp position and the orientation of the dental cast during the deposition and curing of the acrylic. The result is a smooth acrylic base having the appropriate contours and thickness, requiring only minimal trimming and polishing.

The machine employs a system which orients the cast and partially complete appliance to facilitate both the three-dimensional scanning of the dental cast and acrylic deposition and curing. Machine motion, appliance attitude, acrylic flow rate, and ultraviolet light exposure time are regulated to obtain accurate acrylic deposition and to ensure that the liquid does not flow out of the desired shape before it solidifies.

The software to control the system includes machine motion control, a user interface, image processing and process planning functions. The system provides a simple graphic interface which permits technicians to learn its use with minimal training.

The machine performs all appliance manufacturing steps except the bending and positioning of retaining wires and expansion screws and some minor finishing work. The wires are still prepared manually and placed on the dental cast by hand.

Benefits of the Automated Process

The automated process provides at least four direct benefits:

- appliances generated using computer imaging and control will be more accurately produced,

- appliances will be of a more consistent quality since the same acrylic base will be produced for a given cast and shape specification every time,
- labour time required to produce appliances will be substantially reduced, probably by one half or about 15 to 20 minutes per appliance,
- there will be a savings in the quantity of acrylic used since only the required amount is applied to the dental cast.

An indirect benefit of the system is the utilization of an acrylic believed to be without the hazardous effects of the material now commonly in use. These effects include allergenic reactions in patients to the acrylic material, and the irritation of the respiratory tracts of laboratory technicians by the toxic fumes that are produced during curing. The acrylic used in this research is a liquid in uncured form and is solidified through exposure to high intensity ultraviolet light.

Also, the ability to track the development of the dentician through the use of the dental cast map is a possible advantage of the system. By comparing the shape and arrangement of the patient's teeth before and after orthodontic treatment, the orthodontist could evaluate its effectiveness and success. This comparison would be performed aided by the graphics and vision software developed for the system.

Automated production of appliances in dental laboratories will remedy in part the shortage of skilled dental technicians by lessening the training required. It may also cause a structural change within the dental industry. With this system, the researchers expect that dentists will be able to fabricate appliances in their own offices. Appliances will not need to be sent out to orthodontic laboratories to be prepared, as is the common practice today.

Chapter 2

Process Overview

2.1 Orthodontics

The dental arches, jaws, face and cranium form a complex pressure system. Some of the constantly varying forces that effect the formation of the teeth are caused by chewing, the tongue and lips at rest and during speech, swallowing, and the eruption of the teeth themselves. The dentician, which is the position and arrangement of the teeth, is subject to these forces. In fact, the teeth are in a constant state of motion during the development of the occlusion. The occlusion is the relationship between the surfaces of the teeth when they come into contact. The action of the orthodontic appliance is to modify, in one way or another, the natural pressure systems of the dentician to correct the occlusion or shape of the mouth.

The removable orthodontic appliance consists of an acrylic base that fits the shape of the upper or lower mouth. Spring wires are imbedded in the acrylic to secure the appliance to the teeth and to exert forces on the teeth. Some appliances have active plates providing movement of parts of the acrylic base of the appliance with adjustment screws in order to produce forces within the mouth. A photograph of a typical upper-mouth removable orthodontic appliance is shown in Figure 2.1.

Orthodontic appliances are used to move or rotate a single tooth or groups of teeth and to produce improvements in the tooth arrangement and occlusal relations. Several references [6,7] offer a complete survey of the different types of orthodontic appliances,

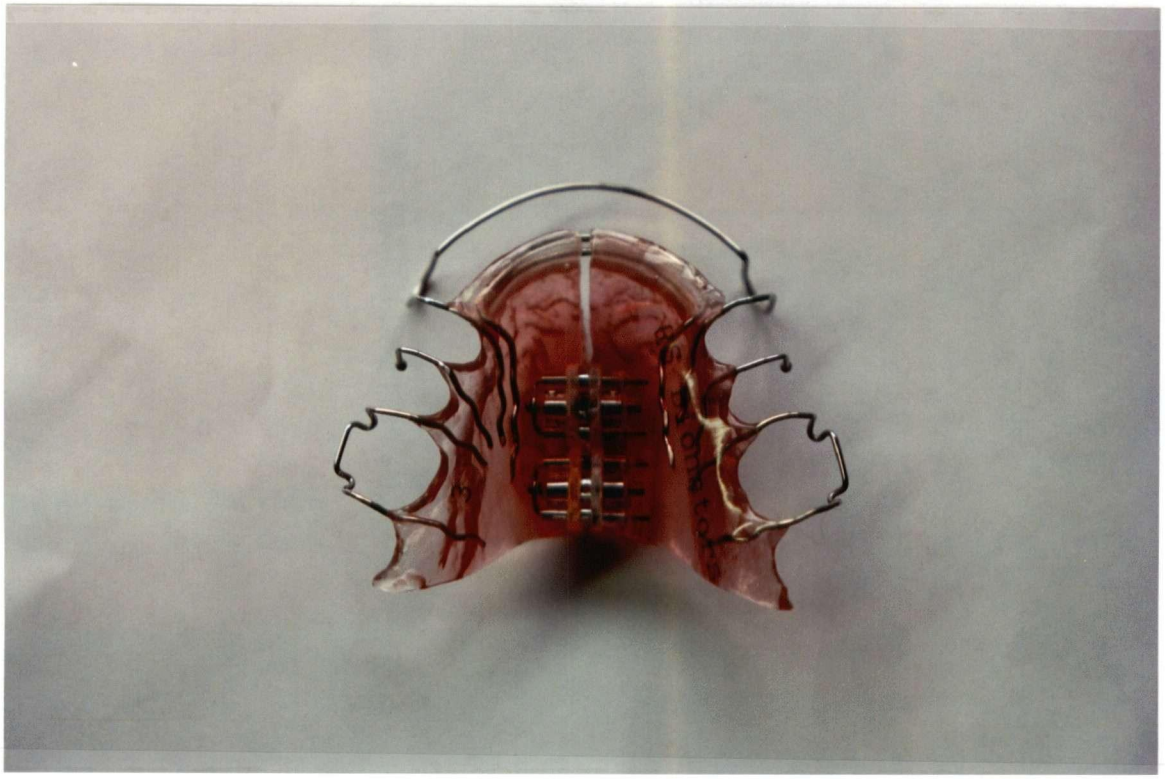

Figure 2.1: Typical removable orthodontic appliance

including their construction and use.

2.2 Current Methods of Manufacture

Currently there are no commercially available advanced systems for the fabrication of orthodontic appliances. The procedure for manufacture is a labour intensive and time consuming task [8]. The manufacturing process can be divided into three major sections: wire bending; acrylic deposition and curing; trimming and finishing.

Before appliance construction begins, the orthodontist makes a rubber mould of the patient's mouth and supplies this to the orthodontic laboratory. The laboratory technician makes a positive mould of the patient's mouth by pouring white plaster or stone plaster into the rubber mould. The cast is used as a base for the appliance construction procedure. Figure 2.2 shows a typical dental cast.

The wires are bent by the technician to suit the particular needs of the patient. After they have been formed, the wires are attached to the dental cast with a small amount of wax. If the appliance has an active plate, expansion screws are also waxed to the cast at the desired position. Also, wax may be applied in order to direct the finished shape of the acrylic material. The cast is soaked in water before the acrylic is applied in order to avoid the formation of air bubbles in the acrylic during curing. The dental cast is also treated with a separating agent to allow removal of the appliance from the dental cast after construction is complete.

The most popular method for acrylic application is the salt and pepper technique. In this process, the material used for the appliance base consists of an acrylic powder and a polymerizing liquid. Colour pigments are also used in order to reduce the visibility of the appliance in the patient's mouth. The powder and liquid are alternatively applied to the cast to form the appliance base. For a good polymerization, the technician must

Figure 2.2: Dental cast made from rubber impression of mouth

ensure that the proper amount of each substance is deposited at each step of the acrylic build-up. After all the acrylic is applied, the appliance is placed in a heat and pressure pot for the final cure. The pot ensures complete cure and low porosity in the appliance.

An alternative method is the light cure system which employs a liquid acrylic that polymerizes under exposure to ultraviolet light. With this manual process, acrylic is repeatedly applied to small sections of the cast and cured under an ultraviolet light source until the complete appliance is formed. No pressure and temperature pot are required.

After the acrylic curing is complete, the appliance is manually trimmed using grinding wheels and acrylic burs. Finishing and polishing are performed on a table-top lathe with various types of coarse to fine polishing compounds using rag and chamois wheels. The finished product must have a lustre appearance and fit comfortably.

2.3 Computer Vision Surface Measurement Techniques

In order to automate the acrylic application procedure, a three-dimensional model of the dental cast surface is required. This section provides a survey of the computer vision technologies that may be applicable to this problem. The survey includes laser radar, moiré fringe, focusing, optical absorbency and active triangulation techniques. Several sources give a thorough review of robot and computer vision methods, see [9,10,11,12, 13,14].

Image sensors

In order to implement a computer vision range-finding system a method of image measurement is necessary. Area charge coupled device (CCD) array based cameras are used most often in image analysis, however other systems including linear CCD arrays, area

resistive gate sensors, area charge injection device (CID) arrays, metal oxide semiconductor dynamic random access memories (MOS DRAM) with optical windows, and position sensitive diodes have been used in range vision scanning systems [10, pp. 130–154].

Laser Radar

Laser radar sensors measure the range of a point by the time of flight of a laser beam. An advantage of this system is that the source and receiver can be close together. The distance at which the radar can operate depends on the intensity of the reflected light in relation to the surroundings.

One method used in measuring range involves emitting short pulses of laser light and waiting for the echo. The transit time is then related to the distance travelled. The depth of field of this type of system depends on the maximum distance that the reflected laser beam can be detected.

Distance can also be found through amplitude modulation of the laser intensity. The range is then proportional to the phase shift between the projected and reflected beams. If no other information about the object being measured is available, the depth of field of this technique is limited to half the modulation wavelength.

Frequency modulation can also be used to measure range with lasers. The transmitted optical frequency of the laser is varied linearly between $(\nu \pm \Delta\nu/2)$ at a frequency of f_m. The range, r, as a function of the beat frequency, f_b, is obtained by mixing the transmitted and returned signal. The range is proportional to the beat frequency as shown in (2.1) [15].

$$r(f_b) = \frac{c f_b}{4 f_m \Delta\nu} \tag{2.1}$$

Moiré Fringe

The moiré fringe technique measures distance visually through interference patterns. Surface elevations are measured by projecting light on to the surface through an optical grating and viewing the reflected light through another similar grating. The interference created by the gratings produces contour lines of equal range from the camera [16]. Sub-contour accuracy based on phase is usually impossible to attain due to differences in intensity inherent in the image.

In the shadow moiré technique, used for surfaces with small depths of field, a single grating is placed close to the surface of interest and the light source and camera use the same grating. In the projection moiré method, two closely matched gratings are used, one for the camera and one for the projector. The gratings are further away from the surface than with the shadow moiré technique and higher depth of field is obtained.

The moiré fringe technique is difficult to automate without further information about the surface since the sign of the slope calculated by the distance between contours cannot be determined. The surface geometry must be smooth with no step changes. Also, the absolute depth to any one contour cannot be calculated from the moiré data.

Focusing

The Gauss thin lens law, (2.2) can be used to relate focal plane distance to object distance [15]. The focal length is f, the distance from the object to the centre of the lens is Z, and the distance from the image plane to the centre of the lens is W. Equation (2.2) can be rewritten as (2.3) to give the focused image plane distance as a function of object distance.

$$\frac{1}{W} + \frac{1}{Z} = \frac{1}{f} \tag{2.2}$$

$$W(Z) = \frac{Zf}{Z - f} \tag{2.3}$$

The blur on the edge of a point viewed at the image plane is a guide to the focus of the camera, the lower the blur, the better the focus. The distance to the point can be found by actively changing the image plane distance to minimize blur. At the point of minimum blur $W = W(Z)$.

Optical Absorbency

Range information can be determined by exploiting the optical attenuation of light through a dissipative medium. If a surface to be measured is immersed in a coloured liquid and the lighting conditions are controlled, the intensity of the image reveals the distance of the surface under the liquid. The object being measured must be consistent in colour and reflectivity for obvious reasons.

Samson et al [17] have developed a system based on this process to measure the surface shape of wax dental implants to accuracies within 0.1 mm as part of a dedicated diagnostic system in orthodontics. The depths measured are relative and do not reveal absolute depths below the surface.

Active Triangulation

The position of a point on a surface can be determined by triangulating between a structured light source illuminating that point and a camera viewing the illuminated point. The position of the camera and the equation for the structured light must be known accurately. This method is easy to implement and is the oldest known method of optical range finding. The disadvantage is that shadowing or occlusion of the view will result in missed range data.

Several types of structured light have been used in active triangulation systems. Point source systems have been developed that use small separations between the source and detector [15].

The next progression from a projected point is a light stripe. By projecting a plane of light, a series of range data points along the incident light on the surface can be obtained. Applications of light stripe range finding systems include robotics and manufacturing automation [18,19,20]. Light stripes can be generated with a cylindrical lens or by the rapid scanning of a light beam so that many point sources pass over the surface during the imaging time. Rapid scanning can be achieved through galvanometer mirrors, reciprocating mirrors, multi-sided rotating mirrors, acousto-optic and electro-optic techniques [10, pp. 154–163]. Most triangulation systems use a camera/laser separation of greater than 45° for good sensitivity. Range vision systems have been used for many biomedical applications including measuring the surface area of the face [21] and the shape of feet [22]. The construction and performance of a laser range-finder with a light stripe source is described in [23].

Several other geometries of structured light have been implemented, including multiple parallel lines and square grids of lines, in an attempt to extract more range data from each image resulting in faster scanning times. However, since there are multiple scan lines in each image, ambiguity about which line corresponds to which elevation can arise. Surface orientation has been calculated by analyzing the orientation of projected geometric shapes including grids and circles, triangles and multiple lines [24,25]. A cross stripe system using two perpendicular planes of light has been suggested for inspection purposes, this method is suitable for Coons' patch surface modeling [26].

Camera Calibration

All these methods require both the intrinsic and extrinsic parameters of the optical sensor, usually a camera, to be calibrated so that the data obtained can be related to the surroundings. The extrinsic parameters describe the position and orientation of the camera with respect to the world coordinate frame whereas the intrinsic parameters describe the internal geometric and optical properties of the camera such as focal length, lens distortion and image origin [27]. A survey of camera calibration techniques is given by Tsai [28]. The methods suggested for three-dimensional computer vision calibrate the camera by analyzing an image that contains known world coordinate data. The image data are compared with the world coordinate data and the intrinsic and extrinsic parameters that best map the data are calculated. The methods vary as to whether linear or non-linear models are used to relate the camera parameters to the world coordinates and in the amount of data required from the image.

Chapter 3

Machine and Process Description

3.1 Functional Specification

The functional and process descriptions for the automated manufacturing of orthodontic appliances are presented in this section. The task description discusses what the machine actually does and the process description states how the task is performed.

3.1.1 Task Description

The purpose of the machine is to fabricate the acrylic bases of orthodontic appliances. As a practical device, the machine must compete with existing manual methods of construction. Therefore, the quality of the appliance made with the automated process must be as good as or better than that produced by current methods. Also, the time required for appliance construction must be competitive with that of the existing process.

The purpose of the acrylic base of the appliance is to imbed the wires and expansion screws and to apply forces to the dentician and surrounding bone structure. The acrylic must cover all the retaining wires and expansion screws. If the acrylic is too thick it will cause discomfort in the patient and possibly restrict breathing. Therefore, the acrylic should be as thin as possible while still covering the wires and expansion screws and having enough strength to apply the required forces. Also, the surface of the acrylic must be smooth so as to avoid irritation of the mouth or tongue.

In current methods of manufacture, much more acrylic is applied and cured than is

actually needed for the appliance. The final shape is obtained by removing the excess with a grinding wheel. The machine developed in this work applies only the required amount of acrylic to the dental cast, thereby eliminating much of the grinding, trimming and buffing work the dental laboratory technician must perform to finish the appliance.

The machine is controlled through a simple user interface that minimizes the amount of operator input required. Two graphical representations of the dental cast are included to help visualize the shape of the appliance. One image is the live camera view of the cast. The second is the computer representation of the cast with image intensity representing elevation, higher elevations being lighter in shade. With these views, the technician can visualize the cast in three dimensions. The operator specifies the desired shape and type of appliance by drawing the outline of the appliance on these graphic images of the dental cast.

The current goal of the machine is to produce removable upper mouth sagittal and transverse orthodontic appliances. The appliances the machine is capable of producing include the following:

- Upper Shwartz Appliances. These appliances have one expansion screw for transverse expansion of the upper mouth.
- Unilateral Sagittal Appliances. These appliances have one expansion screw to move a tooth or a few teeth distally.
- Upper Sagittal Appliances. These appliances have two adjustment screws to expand in the anterior/posterior direction.
- Combination Appliances. These appliances have one transverse and two sagittal expansion screws to provide lateral and sagittal development.

As with existing methods, a plaster cast of the patient's mouth is still required as a base for the manufacture of the appliance. Also, the wire work must still be performed by the dental technician. The expansion screws and wires must be placed on the appliance

by the technician prior to acrylic application.

3.1.2 Process Description

Since the primary function of the machine is to produce the acrylic portion of the appliance, the properties of the acrylic are critical in the choice of manufacturing method. Before curing, the acrylic used in the appliances must be in a form suitable for handling in an automated process. It must also be free of toxic effects for the laboratory technician and the orthodontic patient. Therefore, the analysis of the acrylics considered focuses on these two areas. Two types of acrylic, both currently used in manual methods of appliance construction, were evaluated.

The first type of acrylic considered consists of two parts, a polymethacrylate powder and a methyl-methacrylate monomer liquid. The methyl-methacrylate acts as a solvent, first transforming the powder into a liquid form and then evaporating to cure the acrylic in the desired shape. See [29] for more information on the chemical properties of this material. In current methods using this acrylic, the appliance is produced by first pouring small amounts of powder on to the dental cast in thin layers and then adding solvent to polymerize. The procedure is repeated to form the entire appliance shape. The appliance is then placed in an auto-polymerization heat and pressure pot in order to remove any porosity and cure the acrylic. After curing, excess acrylic is removed through grinding and the appliance is polished to a lustre finish. In orthodontic laboratories, this process is called the salt and pepper technique, referring to the manner of adding a small portion of powder and then a small portion of monomer until the mixture is correct.

The second type of acrylic considered is a liquid before curing, and is cured with exposure to high intensity ultraviolet light. This acrylic consists of oligomer-acrylates mixed with photochemically reactive monomers. See [30,31] for more information on the chemical and curing properties of this acrylic. The available systems using this material

require the acrylic to be squeezed from a tube onto the surface of the cast and then held under an ultraviolet lamp until semi-solid. After approximately five seconds of exposure to the ultraviolet lamp, the acrylic takes on a semi-solid form called the pre-polymerized state. The procedure is repeated on several small areas of the cast to build the entire appliance. Once the complete appliance is pre-polymerized, it is placed under a shorter wavelength ultraviolet lamp for the final cure which takes about three minutes. The shorter wavelength lamp provides deeper curing of the acrylic but must be shielded since it is not eye-safe.

The ultraviolet-cured acrylic was chosen for use in the automated process for several reasons. From a process point of view, it is easier to measure and deposit a liquid than a powder. Also, the liquid acrylic does not require a heat and pressure pot for the final cure. A light source for curing is also easier to position and control than a solvent applicator.

As well, there is concern for the technician and the orthodontic patient over the safety of the methyl-methacrylate monomer used in the salt and pepper technique. Such problems as irritation of the nose, eyes, and skin, drowsiness and unconsciousness at high levels of exposure have been reported. The main toxic effect, however, is irritation of the respiratory tract by exposure to the vapour of the monomer. Dental technicians molding the polymer by hand reportedly developed dermatitis [32]. Some patients using appliances made with methyl methacrylate develop allergies to the acrylic. The solvent based acrylic has the added disadvantage of shrinkage during curing due to the evaporation of the solvent, resulting in an appliance slightly smaller than the cast size. And finally, the ultraviolet cured acrylic does not need the same amount of trimming and buffing as the salt and pepper technique because the liquid acrylic can be applied much more accurately, although a small amount of grinding and polishing is still required to finish the appliance.

With the ultraviolet-cured acrylic, under the current methods of manufacture, the

acrylic work is performed in several stages. Since the surface of the dental cast is highly curved, liquid acrylic could not be applied over the whole area as it would run before it could be cured. The technician holds the dental cast so that the area of application is horizontal, and applies and cures the acrylic at that orientation. Then, the cast is re-oriented so that an adjacent area of application is horizontal and the procedure is repeated, bonding the two sections of acrylic together. A currently available system [33] for the manual preparation of orthodontic appliances with light cured acrylics uses two ultraviolet sources, a high pressure mercury lamp and a Xenon strobe-lamp. The lower frequency mercury lamp is filtered to provide light in eye-safe wavelengths between 360 and 410 nm and is used to pre-polymerize the acrylic. The higher frequency Xenon lamp with wave-lengths from 300 to 350 nm is used for the final cure. The pre-polymerization raises the viscosity of the acrylic to the point that it will no longer flow over the surface. At this point of polymerization additional acrylic can be applied and bonded to the existing work. The pre-polymerization takes approximately 2-3 seconds at a luminous power of 1 W/cm^2. The final cure with the high frequency lamp requires approximately three minutes at a flash power of about 100 W.

The process chosen for the automated production of the acrylic bases mimics the current methods of manual preparation used for the ultraviolet cured acrylic. This involves manipulating the dental cast so that the surface of deposition is horizontal, applying the acrylic over that small area, pre-polymerizing, then re-orienting the cast and repeating the procedure on an adjacent region until the complete appliance form has been made. The wires and retaining screws are still placed on the surface of the dental cast manually before the machine begins the acrylic application process. Wax is used to hold the wires and screws in place during the process. After all the acrylic for the appliance is applied and pre-cured, final curing takes place. Minor grinding around the edges of the appliance is required after the acrylic is cured.

In order to produce appliances in this manner the machine must first determine the shape of the appliance and dental cast. A surface elevation map of the dental cast is obtained using an active non-contact sensor called a range camera. The range camera operates by shining a beam of laser light onto the surface of the dental cast and observing the position of the incident light on the cast with a camera. If the position of the camera and the laser are accurately known, the three-dimensional position of the point on the cast can be calculated. By scanning the entire surface of the cast a full three-dimensional elevation map can be obtained. Surface normals to the dental cast are calculated by fitting curves to the elevation data at localised points on the surface of the cast and taking the normals to the equations of the curves. A least squares fit is used to find the best interpolating plane for the localised surface elevation data. The elevation data are required for tool offset calculations and the surface normal data are required to determine how to orient the cast for acrylic application. A peristaltic pump with a nozzle applicator is used to deliver the liquid acrylic to the surface of the cast and an ultraviolet lamp with a fibre-optic light tube is used to direct the light for curing. The cast is manipulated with a two-axis rotary table and the laser, camera, pump and lamp are moved over the surface of the cast with a two axis linear table. More detail on these components is given in the next section.

3.2 Machine Description

In this section, a detailed description of the machine is presented, including the dental cast manipulation for acrylic application, the surface mapping process, the acrylic deposition and curing procedure, the machine construction, and the electronics and control of the system.

3.2.1 Dental Cast Manipulation

In order to manipulate the appliance so that the surface of deposition is horizontal, a two-axis computer-controlled rotary table system as shown in Figure 3.1 was developed. This robotic manipulator consists of one rotary table mounted on top of another. The axes of rotation of the two stages intersect and the plane of rotation of each stage is mutually perpendicular. The base rotation is used to orient the upper table with respect to horizontal. The upper table, upon which the dental cast is mounted, is used to rotate the point of deposition on the cast to the desired location. Therefore, the device allows the orientation of the cast with two degrees of freedom. This means that the table can only reach a subset of all the possible orientations for the dental cast. However, after considering the shape of the surface of the dental cast where acrylic is applied, this number of axes was considered sufficient. The roof of the mouth when viewed from the back is concave in shape, and tends to be relatively flat at the top with increasing curvature towards the teeth. It is this symmetry that allows the two rotations to orient the cast well enough for acrylic deposition without running. An experiment to determine how close the surface of dental casts can be brought to horizontal using the two-axis rotary table was performed. This analysis is presented in Appendix B.

3.2.2 Dental Cast Surface Mapping

A computer vision system was used to determine the elevation map of the dental cast. The system, shown in Figure 3.2, consists of a CCD camera, a low power (1 mW) helium-neon laser and a high speed (1000 RPM) six sided rotating mirror system. The laser shines onto the rotating mirror system in such a way as to produce a high speed scan of the laser beam across the surface of the dental cast. During the time the CCD camera takes to form an image of the dental cast, several reflected beams scan across its surface.

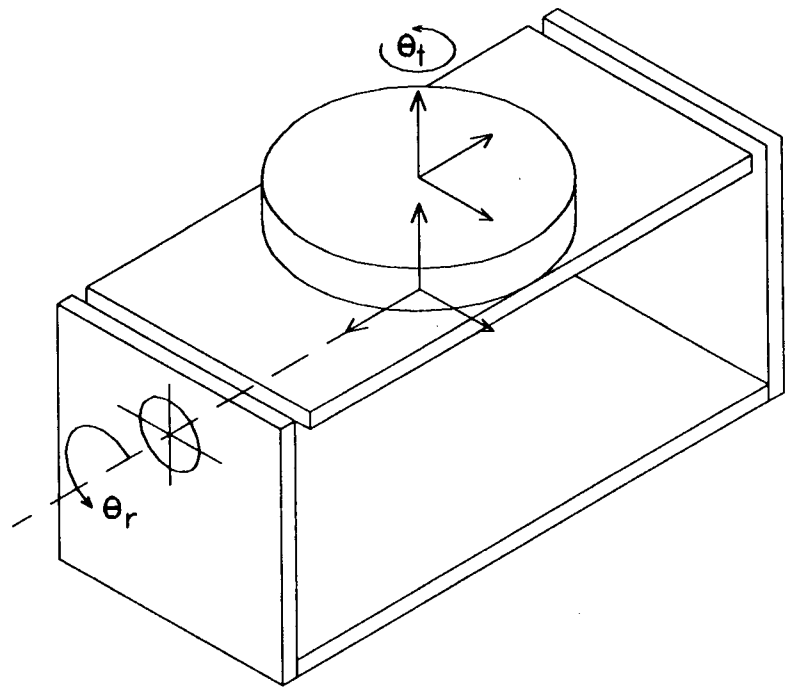

Figure 3.1: Two axis rotary table system for dental cast manipulation

The resulting image from the camera is a stripe of high intensity light along the scan path. By triangulation between the light source and the camera image, the position of the line on the cast that is illuminated by the plane of light can be determined. If the procedure is repeated several times scanning different portions of the cast, a complete map of the surface of the dental cast can be generated. The orientation of the cast for scanning is accomplished using the two axis rotary table system described above. The surface normal for a small area, approximately 4 $mm \times 4$ mm, on the cast can be found by fitting a plane to the data using a least squares fit. The normal to the plane will be the average surface normal for that region.

3.2.3 Acrylic Deposition and Curing

A peristaltic pump driven by a velocity controlled stepper motor is used to deposit the liquid acrylic onto the surface of the dental cast. The pump is able to deliver the acrylic at a rate of 0.32 ml/min. A high intensity ultraviolet light with a wavelength of 365 nm is used to cure the acrylic. The lamp has a fiber-optic conduit to direct the light to the area of curing. The lamp conduit and the pump nozzle are arranged so that the deposition and curing of the acrylic can be performed from the same machine position. After acrylic is applied to the cast, the pump nozzle is lifted slightly to break the line of the liquid acrylic which, due to its surface tension, may still be attached to the nozzle. The lamp is then used to pre-polymerize the material. The liquid acrylic tends to even out over the surface of deposition before it is pre-cured, leaving a smooth finish.

3.2.4 Machine Configuration

A diagram of the machine illustrating its various components is shown in Figure 3.3. The associated coordinate frames and dimensions are shown in Figure 3.4.

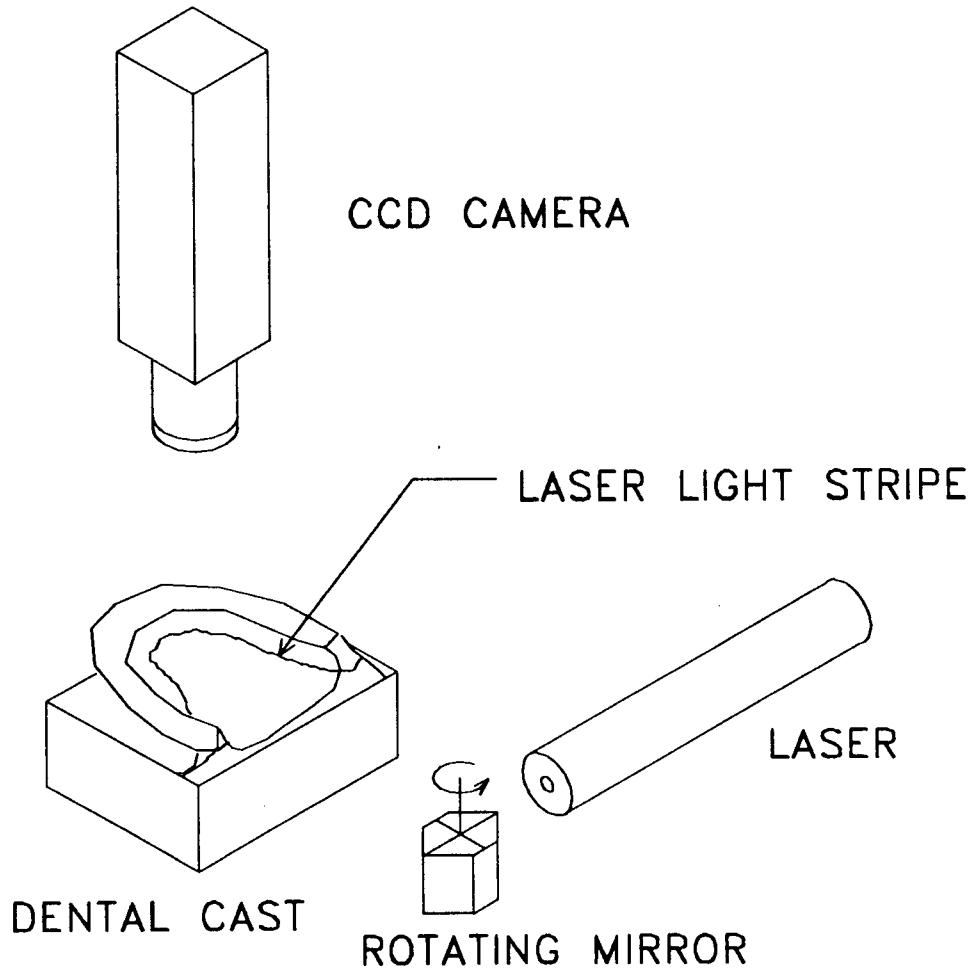

Figure 3.2: Active laser triangulation surface measurement

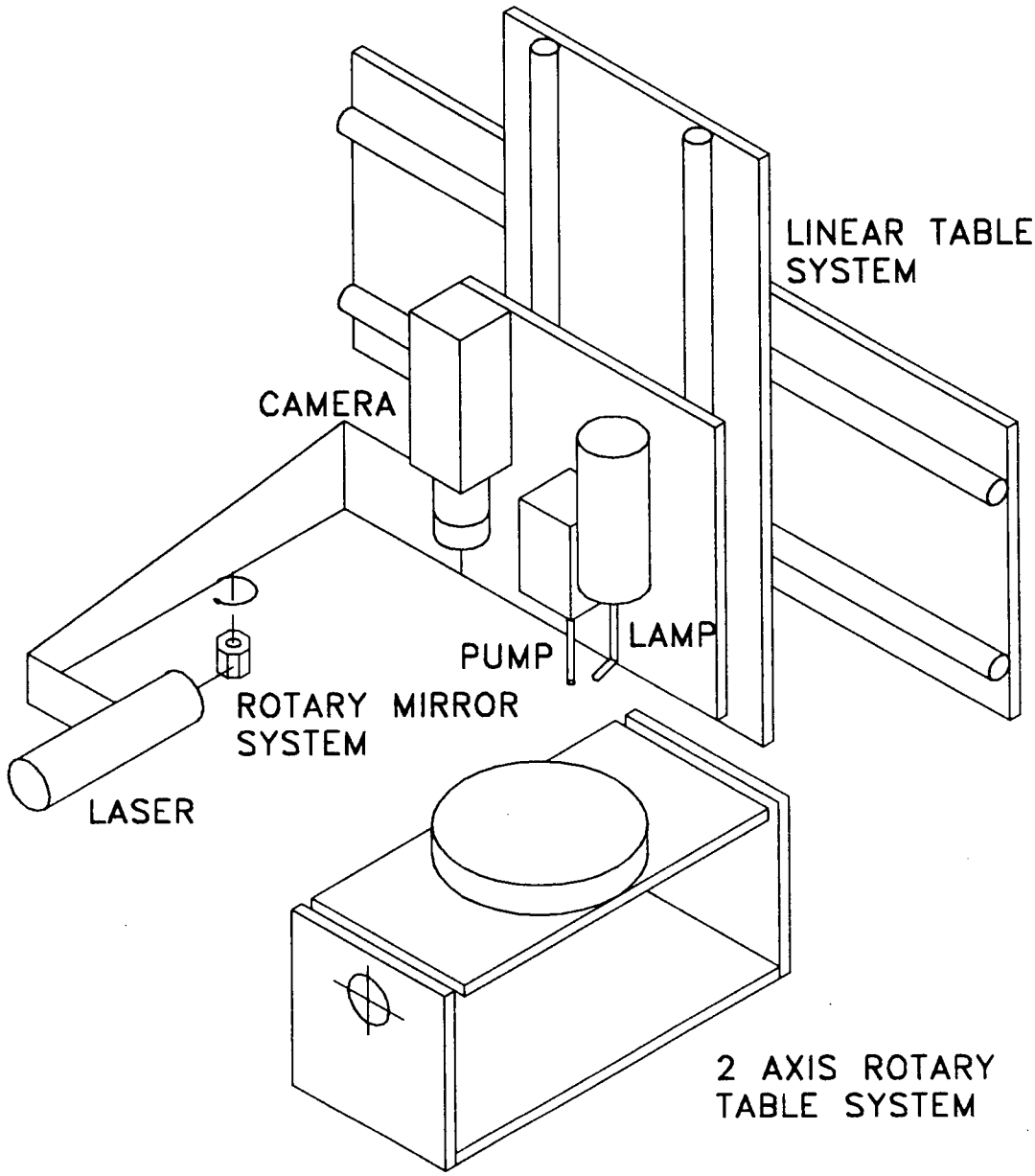

Figure 3.3: Machine components

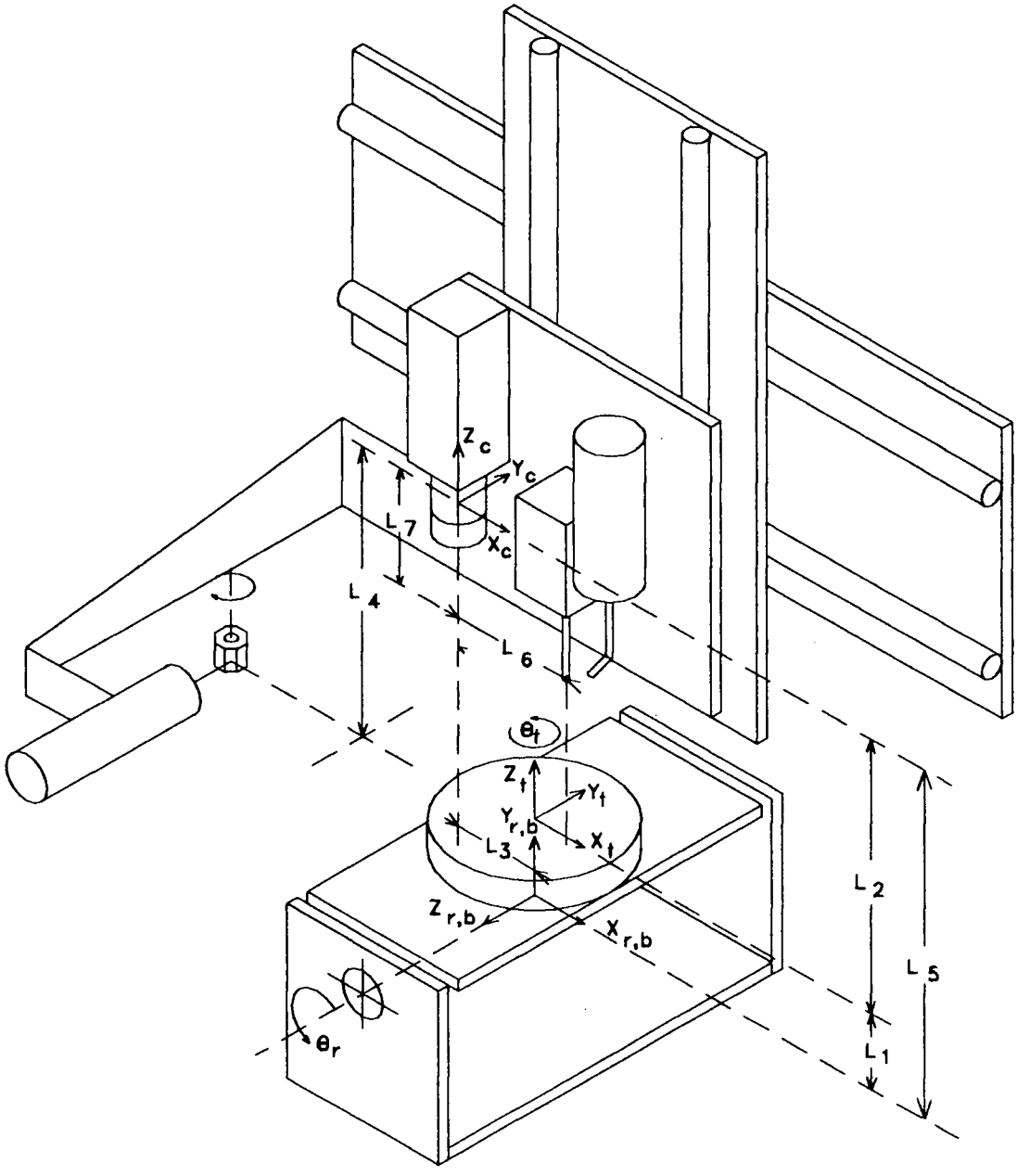

Figure 3.4: Machine with coordinate frames and dimensions

The two linear stages, one mounted horizontally and the other vertically, allow the motion of a table in a vertical plane. Attached to this vertical table (from left to right) are a CCD camera, a peristaltic pump, and an ultraviolet lamp. A laser and rotary mirror system are also attached through an arm on the left-hand side. A two-axis rotary table system, upon which the dental cast is mounted, is positioned under the gantry.

Four coordinate frames are shown on the machine. The base frame, with subscript b, is a stationary frame. The rotary table frame, with subscript r, is shown coincident with the base frame but rotates with the first rotary stage about the Z_b axis. The joint angle parameter θ_r is the clockwise positive angle from the X_b axis to the X_r axis when looking along the positive Z_b axis of the base frame. The table frame, with subscript t, is attached to the table upon which the dental cast is mounted. The origin of the table frame is L_1 along the Y_r axis of the rotary frame. The rotation of the table frame about the Y_r axis is represented by the joint parameter θ_t, the positive clockwise angle from the X_r axis to the X_t axis when looking along onto the Y_r axis. The camera frame, mounted on the vertical motion table, moves in a vertical plane. The origins of all four frames fall in the same vertical plane. The position of the camera frame is represented by two joint parameters, L_3 horizontally from the base frame, and L_5 vertically above the base frame.

The laser and mirror system projects a light stripe a distance L_4 below the camera frame. The plane of the light is perpendicular to the Z_c axis. The nozzle of the acrylic pump is located at the position $(X_c = L_6, Y_c = 0, Z_c = -L_7)$ in the camera frame. The ultraviolet lamp projects light through a fiber optic conduit to a position slightly below the location of the pump nozzle for curing.

3.2.5 Electronics and Control

Figure 3.5 shows the electrical hardware of the machine. An Intel 80386 SX based computer running MS-DOS performs the high level control of the machine. A high

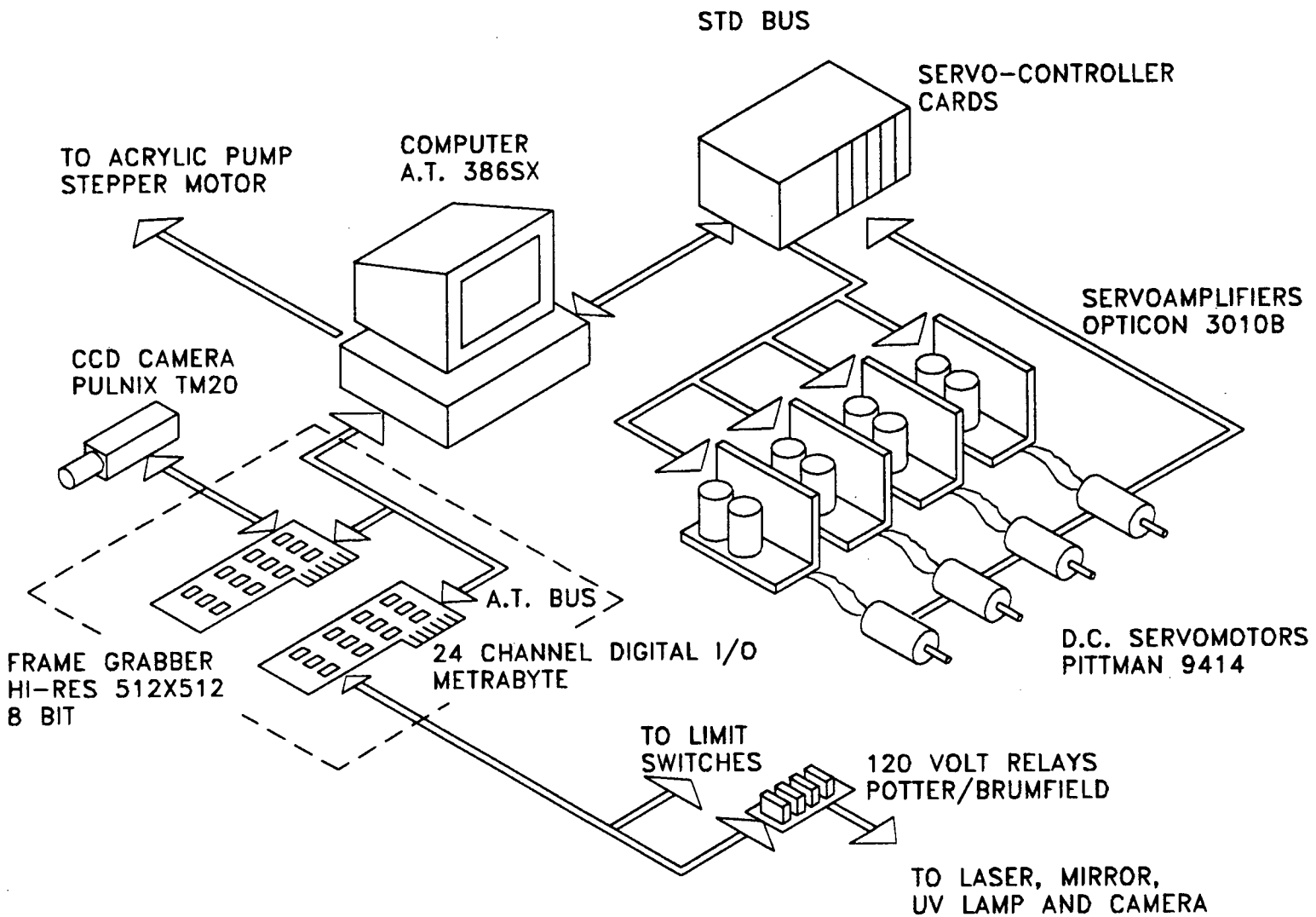

Figure 3.5: Electrical and control flow diagram

resolution (VGA) monitor is used to display live pictures and graphical representations of the dental cast to simplify operator interaction with the system. A pointing device (mouse) is used to enter the desired shape of the orthodontic appliance into the system. The high level system software is written in the C programming language. Intel Assembler is used for time critical and hardware level programming.

A frame grabber card and a 24 channel digital I/O card are installed on the AT bus (shown in the dotted area). The frame grabber board obtains images from the CCD camera and digitizes them into an array of 512 by 512 pixels. Each pixel in the array provides eight bits or 256 levels of intensity data. The 24 channel digital I/O board is used to monitor the limit switches and to control AC power to the various components. The limit switches are used to set the horizontal and vertical gantry axes as well as the base rotational axis to their home positions. The limit switches are placed at the boundary of travel on each axis. The axes are slowly moved until the limit switch is hit and then returned a set distance to their home positions. The home position of the rotary table, which is arbitrary as far as the kinematics are concerned, is set by the operator. The I/O board also controls a set of power relays that control 115 volt AC power to the CCD camera, rotating mirror, ultraviolet lamp and laser.

The servo-controller cards are used to control the DC servo-motors that drive each of the four axes. The controller cards allow constant velocity moves as well as ramped accelerations and decelerations. The cards are housed in an Octagon STD bus card cage. Communication between the AT and STD bus is accomplished through the use of two Ultralink communication cards, one in each bus. The communication cards allow memory and I/O reads and writes between the buses. A diagram of the control loop in Laplace representation for each motor is shown in Figure 3.6. The inputs to the system are the reference input, $\theta_{ref}(s)$, and the torque reflected from the motor shaft, $T_d(s)$. The control law is a digital lead-lag filter with a zero at $-a$, a pole at $-b$, and a

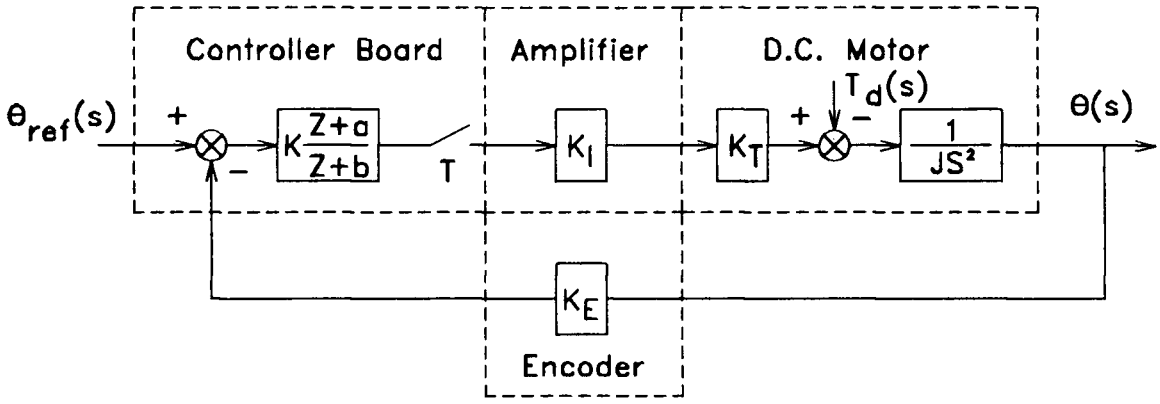

Figure 3.6: D.C. motor control loop

gain of K. The servo-amplifier is a current source amplifier providing a current output proportional to the input voltage from the controller board. The DC motor generates a torque proportional to the input current from the servo-amplifier. The motor output shaft position is measured with an optical encoder and fed back to the controller board. The values of the control loop parameters are given in Table E.1 of Appendix E.

The servomotors driving the rotational axis have a spur gear reduction of 65.5 : 1 on the motor and a further 4 : 1 between the motor and the table. The linear axis have a spur gear reduction of 5 : 1. The leadscrew pitch on the motion tables is 2.54 mm/rev.

The signal to the stepper motor controlling the acrylic pump is obtained from the speaker output on the AT. The speaker is disconnected and the signal is conditioned to allow direct input to the stepper motor driver. The pump speed can be set by programming the frequency of the speaker. The duration of pumping is timed with the internal clock on the computer.

Chapter 4

System Operation

4.1 Kinematics

The forward and inverse kinematics for the machine are developed in this section. The forward kinematics are used for the surface mapping of the dental cast and the inverse kinematics are needed to apply and cure the acrylic material on the surface of the dental cast.

4.1.1 Coordinate Frames

In order to calculate the forward and inverse kinematics for the machine, coordinate frames must be attached to each joint. The orthodontic appliance manufacturing machine consists of two separate kinematic chains: the linear axis gantry, and the rotary table. These chains, each with two degrees of freedom, interact with each other in order to scan the dental cast and apply and cure acrylic. A stationary base frame is used to relate the position of the end effector of one chain with respect to the other.

Referring to Figure 3.4, four coordinate frames, located at the camera, base, first rotary section and the rotary table are used to keep track of the machine position. The camera frame, which is attached to the second linear axis, is used to reference the position of the gantry. All the components mounted on the linear axes are referenced relative to this frame. The transformation between the base and camera frame can be easily determined through geometric analysis. The transformations for the rotary stages are

not so straightforward, however, and a method suggested by both Craig [34, pages 69–77] and Paul [35, pages 101–105] called Denavit-Hartenburg [36] notation was used for assigning the axes to the frames and calculating the coordinate frame relationships.

Under the Denavit-Hartenburg method for rotary frames, the axes are assigned so that the joint rotation for link i takes place about the $\vec{Z}_i$ axis and the $\vec{X}_i$ axis points along a line that intersects the $\vec{Z}_{i+1}$ axis. The $\vec{Y}_i$ axis completes the right hand rule for the coordinate frame. The joints are numbered from the base frame to the end effector starting with frame zero for the base frame. By convention, the base frame is set coincident with frame one when the joint parameter for frame one is zero. Each frame, i, is assigned four parameters a_i, α_i, d_i, θ_i that relate it to the previous and next frames in the chain. The value a_i is defined as the distance from $\vec{Z}_i$ to $\vec{Z}_{i+1}$ measured along $\vec{X}_i$ axis, α_i is defined as the angle between $\vec{Z}_i$ and $\vec{Z}_{i+1}$ measured about the $\vec{X}_i$ axis, d_i is the distance measured from $\vec{X}_{i-1}$ to $\vec{X}_i$ measured along the $\vec{Z}_i$ axis, and θ_i is the angle between $\vec{X}_{i-1}$ and $\vec{X}_i$ measured about $\vec{Z}_i$. By assigning the coordinate frames in this manner, (4.15) in Section 4.1.2 can be used to calculate the transformations. The Denavit-Hartenburg joint parameters for the base, rotary and table frames on the machine are given in Table 4.1.

4.1.2 Transformation of a Point Between Frames

A frame transformation describes the position and orientation of one coordinate frame with respect to another. Consider a system where a coordinate frame is attached to each joint as well as to the stationary base and the end-point of a kinematic linkage. In such a system, the frame transformations between successive links will be a function of the geometry of each joint. By using these transformations, the coordinates of a point whose position is known in one frame can be found in any other frame.

A position is described relative to the frame in which it is referenced. The frame is

written as a leading superscript to the position vector as in (4.1).

$$ {}^{i}P = \begin{bmatrix} P_x \\ P_y \\ P_z \end{bmatrix} \tag{4.1} $$

Where P_x, P_y, P_z are the distances from the origin of frame i to the point P along the X_i, Y_i, Z_i axes.

In order to find the transformation between frames the relative position and orientation of the frames must be known. The position of the origin of frame i relative to frame j is written as a 3x1 vector ${}^{i}P_{jORG}$ as in (4.2). The result of adding ${}^{i}P_{jORG}$ to ${}^{j}P$ is ${}^{i}P$ provided that frames i and j are oriented the same way.

$$ {}^{i}P_{jORG} = \begin{bmatrix} P_x \\ P_y \\ P_z \end{bmatrix} \tag{4.2} $$

The orientation of frame j with respect to frame i is described in the 3×3 rotation matrix ${}^{i}_{j}R$ in (4.3).

$$ {}^{i}_{j}R = \begin{bmatrix} r_{xx} & r_{yx} & r_{zx} \\ r_{xy} & r_{yy} & r_{zy} \\ r_{xz} & r_{yz} & r_{zz} \end{bmatrix} \tag{4.3} $$

Where the directional cosine, r_{uv}, is the projection of the principal axis vector u in the j frame onto the principal axis vector v in the i frame. The rotation matrix relates the coordinates of a point ${}^{i}P$ in frame i with the coordinates of ${}^{j}P$ in frame j as in (4.4). The result of multiplying a position vector ${}^{j}P$ by the rotation ${}^{i}_{j}R$ is ${}^{i}P$ provided that the frames i and j share the same origin.

$$^{i}P = {}^{i}_{j}R\,{}^{j}P \tag{4.4}$$

Equation (4.5) describes how the coordinates of a point in frame i can be found from the description of the same point in frame j and the position and orientation of frame i with respect to frame j. This is a combination of equations (4.2) and (4.4).

$$^{i}P = {}^{i}_{j}R\,{}^{j}P + {}^{i}P_{jORG} \tag{4.5}$$

This is equivalent to first writing ^{j}P in an intermediate frame whose origin is the same as frame j but whose axes are oriented the same way as frame i, and then adding the offset of the origin of frame j from frame i. The rotation and subsequent translation of ^{j}P yields ^{i}P.

In order to simplify the notation, a 4×4 matrix ${}^{i}_{j}T$ is defined that combines the ${}^{i}_{j}R$ and $^{i}P_{jORG}$ matrices as in (4.6). This allows the relation between ^{i}P and ^{j}P to be written as in (4.7). The position vectors are redefined in (4.8) to incorporate the fourth column 1 to yield the new simple notation. All coordinate frame transformations in this thesis use this notation.

$${}^{i}_{j}T = \left[\begin{array}{ccc|c} \multicolumn{3}{c|}{\left[{}^{i}_{j}R\right]} & \left[{}^{i}P_{jORG}\right] \\ \hline 0 & 0 & 0 & 1 \end{array}\right] \tag{4.6}$$

$$\begin{bmatrix} {}^{i}P \\ 1 \end{bmatrix} = {}^{i}_{j}T \begin{bmatrix} {}^{j}P \\ 1 \end{bmatrix} \tag{4.7}$$

$$^{i}P = {}^{i}_{j}T\,{}^{j}P \tag{4.8}$$

4.1.3 Forward Kinematics

In order to build a three dimensional representation of the dental cast in the table coordinate system, each point of data obtained in the camera coordinate frame must be transformed to the table coordinate frame before it can be stored. If the data are stored relative to the table frame, they are independent of the machine position. Referring to Figure 3.4, the quantities L_1 through L_7, θ_r and θ_t describe a unique machine configuration.

During the three dimensional mapping of the dental cast, the cast is manipulated through several orientations. At each orientation, several data points are obtained. The points, however, are obtained in the camera coordinate system and must be transformed to the table coordinate system before they can be added to the surface elevation map. For a specific set of joint positions, the transformations ${}^b_cT$, ${}^b_rT$, ${}^r_tT$ can be calculated. Using these transformations, equations can be written relating the points in camera and table coordinate systems. Equation (4.9) relates a point in the camera frame to a point in the base frame using the camera to base transformation matrix.

$$ {}^bP = {}^b_cT\,{}^cP \tag{4.9} $$

A point in the table frame is transformed to a the base frame by first transforming to the rotational frame and then to the base frame as in (4.10),

$$ {}^bP = {}^b_rT\,{}^r_tT\,{}^tP \tag{4.10} $$

Equation (4.11) is found by equating right-hand sides of (4.9) and (4.10) and solving for ${}^tP$:

$$ {}^tP = {}^r_tT^{-1}\,{}^b_rT^{-1}\,{}^b_cT\,{}^cP \tag{4.11} $$

link	i	a_i	α_i	d_i	θ_i
B	0	0	0°	0	0°
R	1	0	−90°	0	θ_r
T	2	0	0°	L_1	θ_t

Table 4.1: Denavit-Hartenburg parameters

By combining the terms in (4.11) into one transformation from camera to table coordinates the equation can be rewritten as in (4.12).

$$^{t}P = {}^{t}_{c}T\,{}^{c}P \tag{4.12}$$

where,

$$^{t}_{c}T = {}^{r}_{t}T^{-1}\,{}^{b}_{r}T^{-1}\,{}^{b}_{c}T \tag{4.13}$$

The transformation relating a point in the camera frame to a point in the base frame is a linear transformation:

$$^{b}_{c}T = \begin{bmatrix} 1 & 0 & 0 & L_3 \\ 0 & 0 & 1 & L_5 \\ 0 & -1 & 0 & 0 \\ 0 & 0 & 0 & 1 \end{bmatrix} \tag{4.14}$$

The remaining transformations are found using the Denavit-Hartenburg convention. Table 4.1 lists the joint parameters for the base and the first and second rotary axes.

For frames that follow the Denavit-Hartenburg convention, the transformation from one frame to another is governed by (4.15). Note that $C\theta_r = \cos\theta_r$ and $S\theta_t = \sin\theta_t$ etc.

$$
{}^{i+1}_{i}T = \begin{bmatrix} C\theta_i & -S\theta_i & 0 & a_{i-1} \\ S\theta_i C\alpha_{i-1} & C\theta_i C\alpha_{i-1} & -S\alpha_{i-1} & -S\alpha_{i-1} d_i \\ S\theta_i S\alpha_{i-1} & C\theta i S\alpha_{i-1} & C\alpha_{i-1} & C\alpha_{i-1} d_i \\ 0 & 0 & 0 & 1 \end{bmatrix} \tag{4.15}
$$

The transformations ${}^{b}_{r}T$ and ${}^{r}_{t}T$ can be found from (4.15) by substitution of the joint parameters.

$$
{}^{b}_{r}T = \begin{bmatrix} C\theta_r & -S\theta_r & 0 & 0 \\ S\theta_r & C\theta_r & 0 & 0 \\ 0 & 0 & 1 & 0 \\ 0 & 0 & 0 & 1 \end{bmatrix} \tag{4.16}
$$

$$
{}^{r}_{t}T = \begin{bmatrix} C\theta_t & -S\theta_t & 0 & 0 \\ 0 & 0 & 1 & L_1 \\ -S\theta_t & -C\theta_t & 0 & 0 \\ 0 & 0 & 0 & 1 \end{bmatrix} \tag{4.17}
$$

The inverses of these transformations must be calculated in order to evaluate (4.13).

$$
{}^{b}_{r}T^{-1} = \begin{bmatrix} C\theta_r & S\theta_r & 0 & 0 \\ -S\theta_r & C\theta_r & 0 & 0 \\ 0 & 0 & 1 & 0 \\ 0 & 0 & 0 & 1 \end{bmatrix} \tag{4.18}
$$

$$
{}^{r}_{t}T^{-1} = \begin{bmatrix} C\theta_t & 0 & -S\theta_t & 0 \\ -S\theta_t & 0 & -C\theta_t & 0 \\ 0 & 1 & 0 & -L_1 \\ 0 & 0 & 0 & 1 \end{bmatrix} \tag{4.19}
$$

Substituting the transformations into (4.13) and simplifying, we obtain

$$
{}^{t}_{c}T = \begin{bmatrix} C\theta_r C\theta_t & S\theta_t & S\theta_r C\theta_t & L_3 C\theta_r C\theta_t + L_5 S\theta_r C\theta_t \\ -C\theta_r S\theta_t & C\theta_t & -S\theta_r S\theta_t & -L_3 C\theta_r S\theta_t - L_5 S\theta_r S\theta_t \\ -S\theta_r & 0 & C\theta_r & -L_3 S\theta_r + L_5 C\theta_r - L_1 \\ 0 & 0 & 0 & 1 \end{bmatrix} \tag{4.20}
$$

Also, ${}^{c}_{t}T$ can be found from the inverse of (4.20).

$$
{}^{c}_{t}T = \begin{bmatrix} C\theta_r C\theta_t & -C\theta_r S\theta_t & -S\theta_r & -L_1 S\theta_r - L_3 \\ S\theta_t & C\theta_t & 0 & 0 \\ S\theta_r C\theta_t & -S\theta_r S\theta_t & C\theta_r & L_1 C\theta_r - L_5 \\ 0 & 0 & 0 & 1 \end{bmatrix} \tag{4.21}
$$

4.2 Inverse Kinematics

The inverse kinematic problem must be solved in order to apply and pre-cure acrylic on the surface of the dental cast. The four joint positions, $\theta_r, \theta_t, L_3, L_5$, must be found that will position the acrylic pump and lamp over the point of application and orient the cast so that the surface of application is horizontal. The inverse kinematic problem is solved by first finding the joint parameters θ_r and θ_t, and then L_3 and L_5. The rotary axis is used to position the surface normal at the point of acrylic application as close to vertical as possible. The table axis is used to position the point of application in the workspace of the pump and ultraviolet lamp. The two linear axes are positioned so that the pump and acrylic lamp are directly over the desired point of application.

Note that there are, in general, two solutions for the angles θ_t and θ_r that will position the point of acrylic application in the workspace of the pump and ultraviolet lamp and orient the surface normal at the same angle with respect to the Z_c axis. These are (θ_r, θ_t)

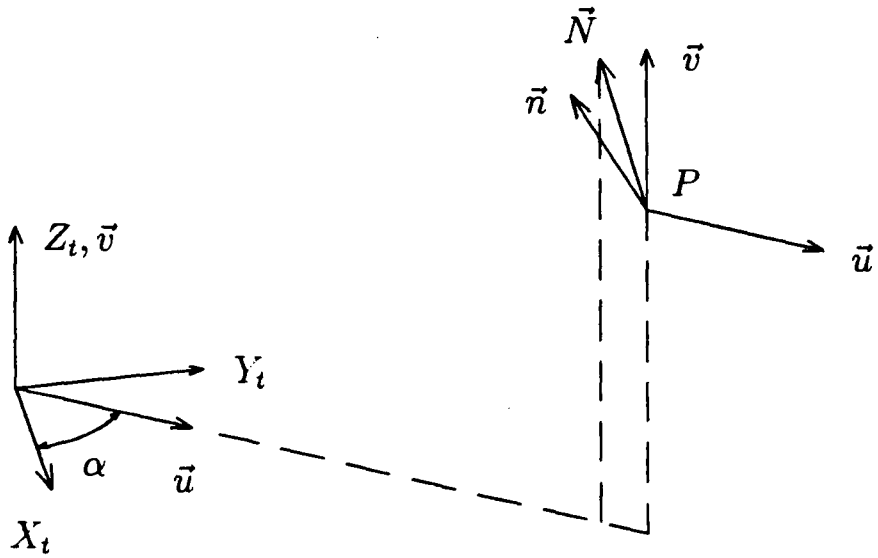

Figure 4.1: Determining the in plane normal $\vec{N}$

and $(-\theta_r, \theta_t + \pi)$. However, the position of the ultraviolet lamp with respect to the pump nozzle dictates that for application and curing $\theta_r \leq 0$. This condition causes the light to fall more incident on the cast surface than $\theta_r \geq 0$ would allow. The disadvantage of this restriction is that large rotations of θ_t may be required when the nozzle trajectory passes close to the origin of the table coordinate system.

4.2.1 Determination of θ_r and θ_t

The joint angle, θ_r, must be found that will orient the surface normal at the point of acrylic application as close to vertical as possible. This is required to avoid the running of the liquid acrylic before it can be cured. In Figure 4.1 the table coordinate frame is shown along with a desired point, P, of acrylic application. The orthogonal vectors $\vec{u}$ and $\vec{v}$ are defined in (4.22) and (4.23). These vectors describe the plane that is the workspace of the acrylic pump and ultraviolet lamp once θ_t has been rotated to the desired position for acrylic application. The angle α is the angle from the X_t axis to $\vec{u}$. In general, the true surface normal $\vec{n}$ is not in the $\vec{u}, \vec{v}$ plane. The vector $\vec{N}$, called the in-plane normal,

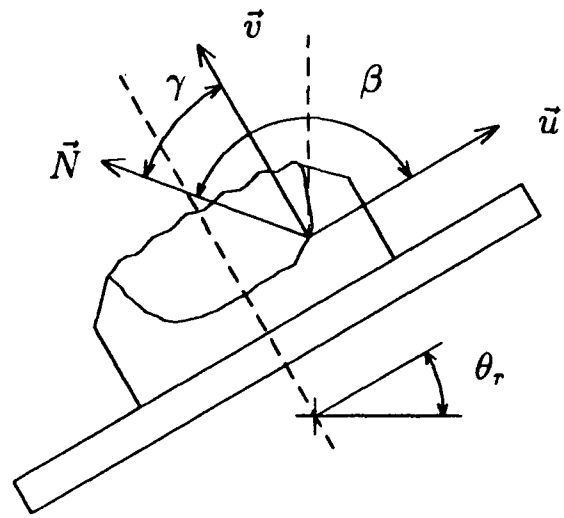

Figure 4.2: Determining the rotation θ_r

represents the closest vector to $\vec{n}$ that is in the workspace of the pump and lamp. The in-plane normal is the nearest vector to the actual surface normal that can be oriented vertically by the two degrees of freedom available in the rotary stages. The vector $\vec{N}$ can be calculated by summing the projections of $\vec{n}$ on to the vectors $\vec{u}$ and $\vec{v}$ as shown in (4.24).

$$\vec{v} = 1\,\vec{k} \tag{4.22}$$

$$\vec{u} = {}^{t}P_x\,\vec{i} + {}^{t}P_y\,\vec{j} \tag{4.23}$$

$$\vec{N} = \left(\frac{\vec{n}\cdot\vec{u}}{\vec{u}\cdot\vec{u}}\right)\vec{u} + (\vec{n}\cdot\vec{v})\vec{v} \tag{4.24}$$

Figure 4.2 is a view of the table and dental cast looking towards the origin of the rotational frame directly along the axis of rotation of θ_r. The angles to the in-plane normal, $\vec{N}$, from $\vec{u}$ and $\vec{v}$ are β and γ respectively. The current position of the table, θ_r, is

shown. The angles α, γ and β are calculated as shown in equations (4.25) through (4.27). In order to orient $\vec{N}$ vertically, the rotary axis joint parameter, θ_r, must equal $-\gamma$.

$$\tan\alpha = \frac{{}^tP_y}{{}^tP_x} \tag{4.25}$$

$$\cos\beta = \frac{\vec{N}\cdot\vec{u}}{\left|\vec{N}\right|\,|\vec{u}|} \tag{4.26}$$

$$\cos\gamma = \frac{\vec{N}\cdot\vec{v}}{\left|\vec{N}\right|\,|\vec{v}|} \tag{4.27}$$

Once the joint angle, θ_r is set as shown in (4.28), the angle θ_t must be found. From this position, there are two angles of θ_t, $-\alpha$ and $\pi-\alpha$, that will rotate P into the workspace of the pump and lamp. One of these rotations, however, will position $\vec{N}$ vertically and the other will position it horizontally. The correct rotation is determined by considering the sign of $\cos\beta$ as shown in (4.29).

$$\theta_r = -\gamma \tag{4.28}$$

$$\theta_t = \begin{cases} \pi-\alpha & \cos\beta \geq 0 \\ -\alpha & \cos\beta < 0 \end{cases} \tag{4.29}$$

4.2.2 Determination of L_3 and L_5

The linear joint parameters L_3 and L_5 must be found to position the acrylic nozzle a distance Z_{coff} directly above the point P when θ_r and θ_t have been positioned so as to orient $\vec{N}$ vertically. The vector ${}^cP$ can be found from ${}^tP$ using the transformation ${}^c_tT$ as given in (4.21).

$$^{c}P = {}^{c}_{t}T\,{}^{t}P \tag{4.30}$$

After ^{c}P has been found, the required joint movements are apparent from the geometry of the machine.

$$\Delta L_3 = -L_6 - {}^{c}P_x \tag{4.31}$$

$$\Delta L_5 = -L_7 - Z_{coff} - {}^{c}P_z \tag{4.32}$$

The amount by which the pump nozzle applicator is offset from the surface of the dental cast is Z_{coff}.

4.3 Dental Cast Surface Mapping

4.3.1 Overview

Since each dental cast is different, the machine must determine the shape of the dental cast before an appliance can be made. A map of the elevation and surface normal of each point on the cast is required before the deposition and curing of the acrylic can occur. The surface normal data is required to position the cast so that the liquid acrylic does not run when it is applied. The elevation data are required for tool offset calculations in both the application and curing process.

The method chosen to obtain the surface elevation data involves the use of structured light and a computer vision system. The components are shown in Figure 3.4. A CCD (charge coupled device) camera is attached to the gantry and is aligned vertically. The position of the camera frame, which is attached to the camera, in relation to the stationary base frame is represented by the distance L_5 in the Y_b direction and L_3 in the X_b direction.

A laser and a six-sided rotating mirror are also attached to the gantry. The laser shines on to the mirror surface at an angle that produces, upon rotation, a plane of light perpendicular to the camera Z_c axis.

When the plane of laser light intersects the dental cast, it generates a line of constant elevation in the camera coordinate frame that can be analyzed by the computer vision system. Points on this line all share the common coordinate ${}^cP_z = -L_4$. If the camera is calibrated at this distance, it is also possible to obtain the ${}^cP_x$ and ${}^cP_y$ coordinates of these points. The entire surface of the dental cast can be mapped by repeating this procedure several times using different combinations of laser elevation and dental cast orientation to ensure full coverage of the surface.

Once the surface elevation of the dental cast has been mapped, surface normals can be calculated. As stated above, the surface normal data are used to orient the dental cast for acrylic application. This procedure involves pumping acrylic onto a small area of the dental cast and then curing. It is therefore advantageous to have the average surface normal for that area. To calculate this, the elevation data array is divided into a rectangular grid of squares, each with an area of approximately 16 mm^2. For each section of the grid a plane is fitted to the data using the least squares method. The normal to this plane is used as the average surface normal for that region.

Since the dental cast is attached to the rotary table on the machine, the surface shape data are stored relative to the table coordinate system. The surface elevation data are found in the camera coordinate system and transformed into this system. This data can be found in any other coordinate system through a transformation.

4.3.2 Image Processing

Each laser scan image contains intensity data for the whole field of view of the CCD camera. The image processing system must analyze this data to determine the position

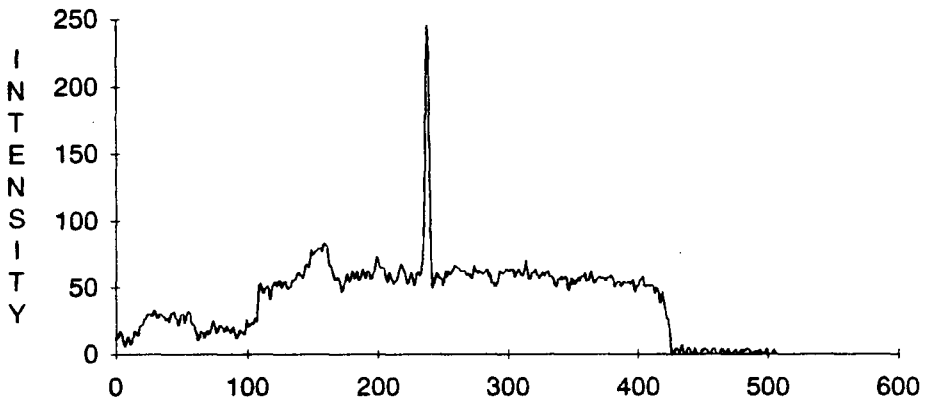

Figure 4.3: Pixel intensity for one column

of the laser scan line. This data, represented as discrete points on the CCD array, are then translated into coordinates in the camera coordinate system. Then, for the specific set of axis positions used for that scan, the data are transformed into the table coordinate system and added to the existing elevation data. The table coordinate system is the only frame in which the data are independent of axis position. If the data were stored in any other frame, the vector positions of the data points would be a function of machine position.

The image is processed into digital form by a frame grabber board and stored as an array in the memory of the host computer. The camera image data are organized as a 512×512 array of cells. Each cell corresponds to a CCD array element and contains one of 256 possible values that represent the light intensity at that element. The image processing software uses the intensity data to find the set of $({}^{p}P_x, {}^{p}P_y)$ data points that contain the intersection of the laser plane and the dental cast.

Figure 4.3 shows the pixel intensity data for one column of pixels in the CCD array.

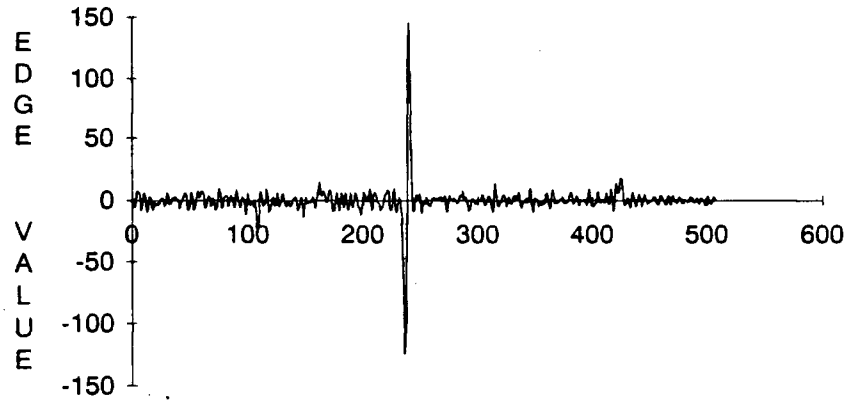

Figure 4.4: Data processed with derivative operator

This is a cross-section of the image intensity data through the image. The horizontal axis is the pixel position in the CCD array and the vertical axis is the image intensity at that pixel location. The large peak in the data represents where the laser scan line crosses the section. Both the slope and the intensity of this peak can be used by the image processing software to identify it as the laser scan line.

A digital rectangle operator was used to compute the slope of the intensity data as suggested by Gonzalez et al [12, pp. 331–390] and Asada et al [24]. Figure 4.4 is the convolution of the data in Figure 4.3 with the rectangle operator $[1, 0, -1]$. The result is a measure of the first derivative of the image intensity data. Note that the value calculated has a sign opposite to the actual derivative and the value is not normalized with the horizontal pixel length. This representation is calculated by subtracting the next pixel location intensity from the previous pixel intensity for each cell on the section. Equation 4.33 illustrates how to calculate the derivative representation, where $S(i)$ is a measure of the slope and $I(i)$ is the pixel intensity.

$$S(i) = I(i-1) - I(i+1) \tag{4.33}$$

This operator has the effect of removing the low frequency transitions and D.C. offset in the data. The height of the peak in the filtered data represents the difference in intensity between the laser scan and the surroundings. The start of the negative peak in the data is the first edge of the laser scan line and the end of the positive peak is the second edge. The width of the scan line in pixels is calculated as the positive difference between the two edge pixel locations. The height of the peak in the data is compared with a threshold level to decide whether the peak represents a laser scan line or simply a change in intensity over the image. The point that must be used to calculate the elevation data is the centre of the laser scan line. The centre is calculated by taking the average of the two pixel edge locations.

The actual centre of the laser scan line is more accurately found when the section is taken perpendicular to the length of the scan line. Figure 4.5 shows two different sections taken through a scan line. The vertical section, which is close to perpendicular, yields an accurate centre value. If the vertical section were taken anywhere in the neighborhood of this point the result would still be accurate. The horizontal section, however, is not accurate. A different and inaccurate centre value is found at different elevations. For a uniform scan line the section that has the least width will be the closest to a perpendicular section. To minimize this effect without increasing the computation too much, each image is scanned once horizontally and once vertically. For each point found, a measure of the width of the laser scan line are stored along with the elevation data for that point. If on a future scan, elevation data is found for the same point, the width of the new scan is compared with the current data. The data point is only overwritten if the new scan width is shorter.

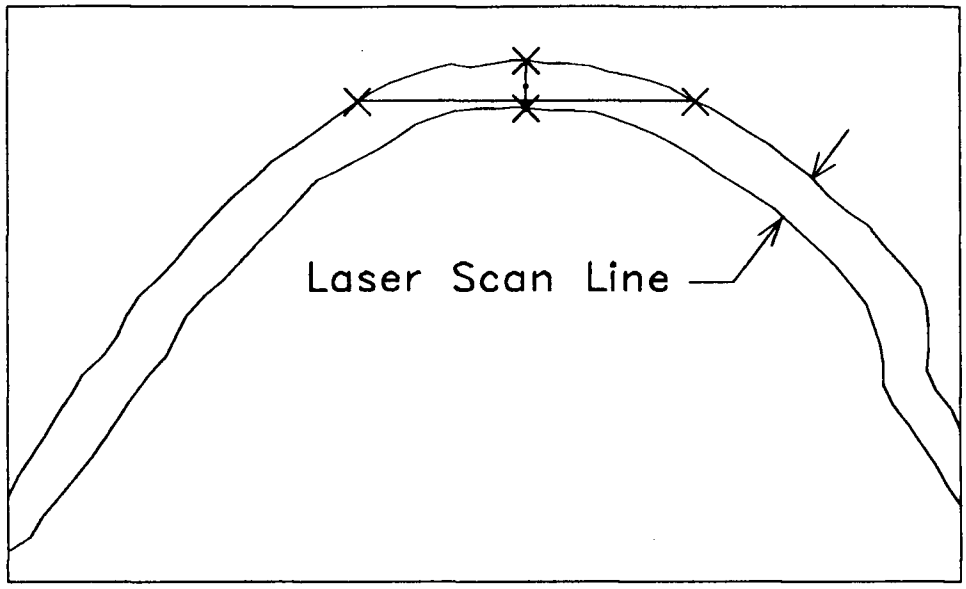

Figure 4.5: Midpoint accuracy versus scan section width

4.3.3 Data Transformation and Storage

This section describes how the elevation data obtained from the camera and laser system is stored in the computer memory. As mentioned in the overview, the elevation data are obtained in the camera coordinate frame. The data is transformed from the camera to table frame were the data point coordinates are independent of machine position. Once in the table coordinate system, the data must be stored in the computer. This section discusses how these transformations are performed and how the data are stored in computer memory.

For each data point, the camera pixel coordinates ${}^{p}P_x$ and ${}^{p}P_y$ are converted to the camera frame coordinates ${}^{c}P_x$ and ${}^{c}P_y$ using (4.34) and (4.35). The ${}^{c}P_z$ coordinate, needed to complete the position vector to the point in camera frame coordinates is a constant as shown in (4.36). In these equations, N_p is the number of rows and columns of pixels in the CCD array. S_c is the calibration factor in $[mm/pixel]$ in the ${}^{c}P_x$ and ${}^{c}P_y$

directions for the camera at the distance of the laser scan line. This scale factor is found experimentally by counting the pixel length of a line of known length a distance L_4 from the camera. C_{yoff} is the distance from the origin of the camera coordinate frame to the centre pixel of the CCD array in the Y_c direction in pixels. This distance is found by viewing the centre of the table through the camera and counting the camera pixels from the centre of the CCD array to the centre of the table. The offset of the camera in the X_c direction is set to zero by controlling the home position of the L_3 axis.

$$^{c}P_x = (N_p/2 - {}^{p}P_x)S_c \tag{4.34}$$

$$^{c}P_y = ({}^{p}P_y - N_P/2 - C_{yoff})S_c \tag{4.35}$$

$$^{c}P_z = -L_4 \tag{4.36}$$

Before the dental cast is mapped, the technician enters some basic cast sizes into the system. These include the total width of the dental cast, C_{wid}, the total length of the cast, C_{len}, the maximum height at the front, C_{zmax}, the minimum scanned height, C_{zmin}, the distance from the back of the cast to the table frame coordinate origin, C_{bc}, and the height at the back of the cast, C_{zb}. These distances are used to maximize the resolution of the stored elevation data and to decide which elevation sections should be used to scan the cast. These dimensions are shown in Figure (4.6). In reality, C_{zmin} should be chosen slightly less than the actual minimum scanned height to ensure that the minimum cast height will be represented in the elevation map.

The position vector ^{c}P in the camera coordinate frame can be transformed to the table coordinate frame using the transformation $^{t}_{c}T$ defined in (4.20).

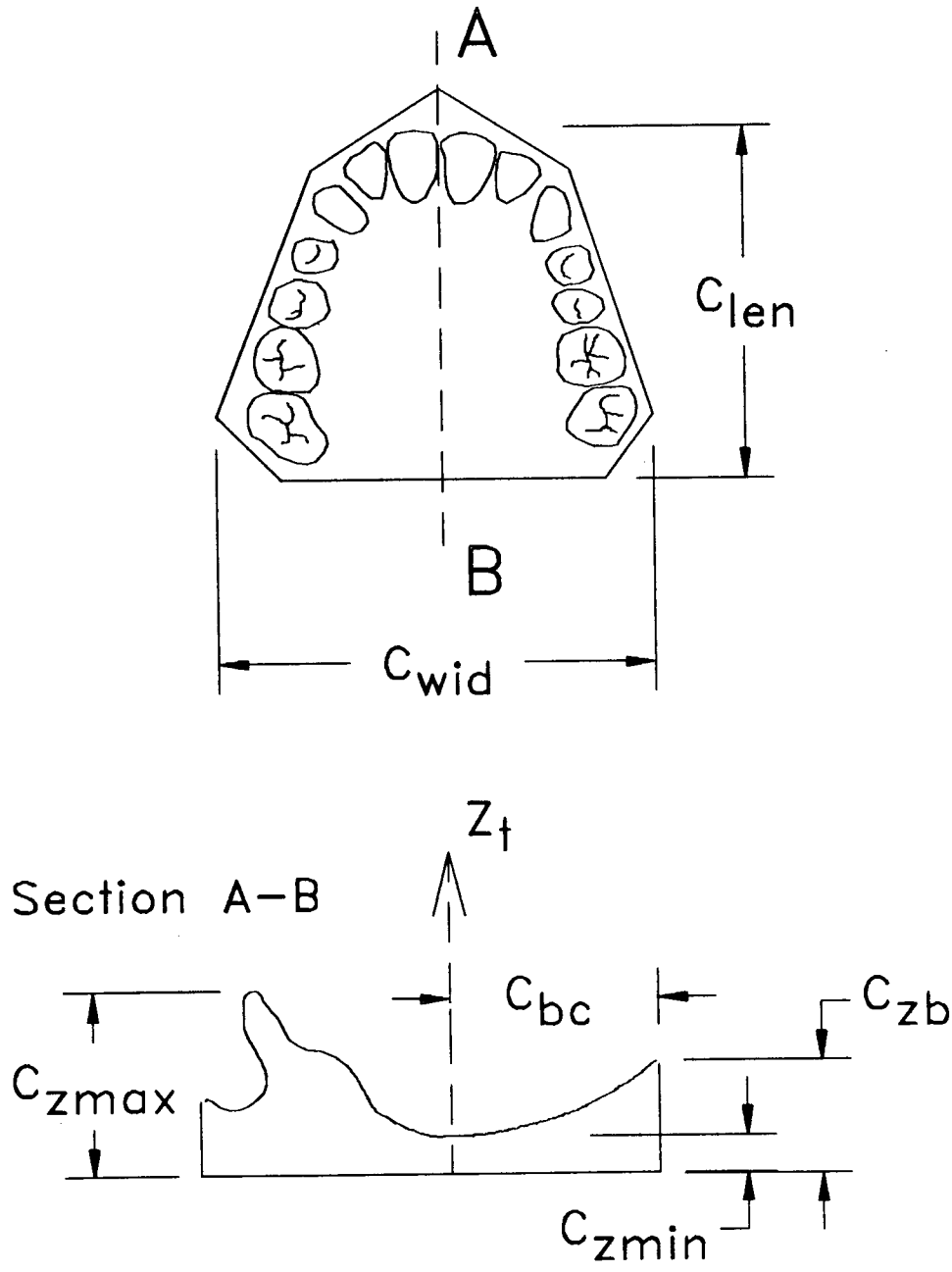

Figure 4.6: Basic cast dimensions

$$^{t}P = {}^{t}_{c}T\,{}^{c}P \tag{4.37}$$

Once the position vector has been found in table coordinates it can be stored in the computer memory. The data are stored in an array in computer memory as a range map. The range map is a two-dimensional array, each cell location in the array maps to an $({}^{t}X, {}^{t}Y)$ coordinate in the table frame. The cell value maps to a Z_t elevation in the table frame. The side length of the range map array in cells is N_{mxy}. The coordinate of the array cell is calculated from the ${}^{t}P_x$ and ${}^{t}P_y$ coordinates. The array cell value is calculated from the ${}^{t}P_z$ coordinate. The discrete number of elevations that can be represented in computer memory is N_{mz}.

The scale factors S_{mxy} and S_{mz} are calculated using (4.38) and (4.39). The indices ${}^{m}P_x$ and ${}^{m}P_y$ are the map indices for the data storage array and are found using (4.40) and (4.41). S_{mxy} is the scale factor relating array indices to table coordinates. N_{mxy} is the side length in cells of the array used to store the elevation data in the processor memory. The elevation in table coordinates is stored as the value ${}^{m}P_z$ shown in (4.42). The offset C_{zmin} in (4.42) is chosen to be slightly less than the minimum elevation of interest on the surface of the cast. The scale factor S_{mz} relates the cast elevation to the cell value.

$$S_{mxy} = (C_{wid} + 6.4\ mm)/N_{mxy} \tag{4.38}$$

$$S_{mz} = (C_{zmax} - C_{zmin})/N_{mz} \tag{4.39}$$

$$^{m}P_x = {}^{t}P_x/S_{mxy} + N_{mxy}/2 \tag{4.40}$$

$$^{m}P_y = {}^{t}P_y/S_{mxy} + N_{mxy}/2 \tag{4.41}$$

$$^{m}P_z = ({}^{t}P_z - C_{zmin})/S_{mz} \tag{4.42}$$

Section 4.3.2 shows that the calculation of laser scan line midpoint location will be more accurate when the section is taken perpendicular scan line. Sections taken perpendicular to the scan line will yield shorter laser line thicknesses than sections taken at other orientations. This concept is used to improve the accuracy of the elevation data when more than one scan maps to the same cell in the range map. To implement this, an array keeps track of the thickness of the scan line used to calculate the elevation stored in each cell. If the same point is scanned more than once, the thickness of the new scan width is checked against the currently stored value. The value is only replaced if the scan width of the new section is smaller. The width array uses two binary bits of data for each cell. Of the four states that can be represented, one indicates that the cell has not been scanned and the other three indicate decreasing scan width ranges as shown in Table 4.2. Each scan is categorized into one of the three width categories. If the category for the new scan represents a width less than that for the existing scan value, the new data are considered more accurate and the previous data are overwritten. When the inverse kinematics are calculated for material deposition this database is referenced to see if the elevation for the point of deposition is valid, if not the closest valid data point is used instead.

4.3.4 Surface Normal Calculation

The average surface normal is required to orient the dental cast for acrylic deposition. The rotary axes should be oriented so that the surface normal for the region of application

Scan Category	Bit Representation (binary)
Not Scanned or $width > W_0$	00
$W_1 > width \leq W_0$	01
$W_2 > width \leq W_1$	10
$width < W_2$	11

Table 4.2: Scan width database categories and representation

is as close to vertical as possible. This minimizes the possibility that the acrylic will run before it can be cured.

After the surface elevation data for the dental cast has been mapped, the range map representing the elevations on the cast is used to calculate surface normals. The range map data are subdivided into several smaller squares of elevation data. Each axis of the range data is split into N_{grid} portions to form N_{grid} by N_{grid} squares over the entire range map. Some of these squares do not contain any elevation data since they do not cover the cast surface. For the squares that do contain range data, the equation of a plane that fits the data in the least-squares sense is determined. The vector normal to this plane is then used as the surface normal for that portion of the elevation map.

The coefficients a_1,a_2,a_3 for the plane in (4.43) can be found using a least squares fit on the surface elevation data. The least squared plane fit is calculated by solving the set of equations (4.45) through (4.47). For each region, a plane surface is fit to the data. The normal to the plane is the average surface normal for that region and is given in (4.44). A more detailed discussion of least-squared surface fitting is given by Lancaster [37, pp. 146–151].

$$p(x, y) = a_1 + a_2 x + a_3 y \tag{4.43}$$

$$\vec{n} = -a_2\vec{i} - a_3\vec{j} + \vec{k} \tag{4.44}$$

$$(N+1)a_1 + (\sum x_i)a_2 + (\sum y_i)a_3 = \sum f_i \tag{4.45}$$

$$(\sum x_i)a_1 + (\sum x_i^2)a_2 + (\sum x_i y_i)a_3 = \sum x_i f_i \tag{4.46}$$

$$(\sum y_i)a_1 + (\sum x_i y_i)a_2 + (\sum y_i^2)a_3 = \sum y_i f_i \tag{4.47}$$

4.4 Trajectory Planning and Generation

This section describes the methods used to plan the machine motions for the application of acrylic to form an orthodontic appliance. This problem includes deciding where acrylic should be applied and the order of its application on the cast. Since the machine consists of two separate kinematic chains, collisions are possible during the motion of the axes. A method for the avoidance of collisions during acrylic deposition is also presented.

4.4.1 Path Planning

After the elevation and surface normal data have been calculated for the dental cast, the operator must enter the desired shape of the appliance. Two images of the dental cast, as seen from vertically above, are shown on the computer screen. The first is an elevation map of the cast using intensity to represent elevation. The second is a live video image of the cast through the camera on the machine. Cross-hairs are shown on both images as the technician outlines the shape of the desired appliance. A pointing device (mouse) is used to outline the shape of the appliance with a series of straight line segments. The

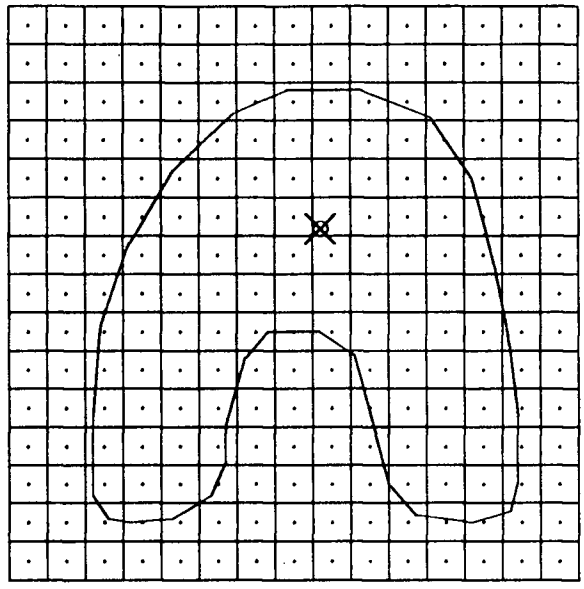

Figure 4.7: Cast outline superimposed on grid map

final outline is a continuous path of straight line segments. Also, one point on the interior of the appliance shape must be indicated.

Figure 4.7 shows an outline of an appliance superimposed over the grid map of surface normal data. For each square in the grid, a surface normal has been calculated by taking the normal to a least squares surface fit of the elevation data inside that square. The path planing software first determines the squares that fall within the desired appliance shape. This is accomplished by constructing a line from a point known to be on the interior of the appliance to the centre of a grid square, and then calculating the number of intersections between that line and the outline of the appliance. This is repeated for every square on the grid. If no intersections or an even number of intersections are found, the grid square is within the outline of the appliance. Acrylic is applied to all the grid squares found within the appliance outline. If the grid is fine enough, the acrylic applied to the squares that are only partially within the appliance shape flows to form a smooth

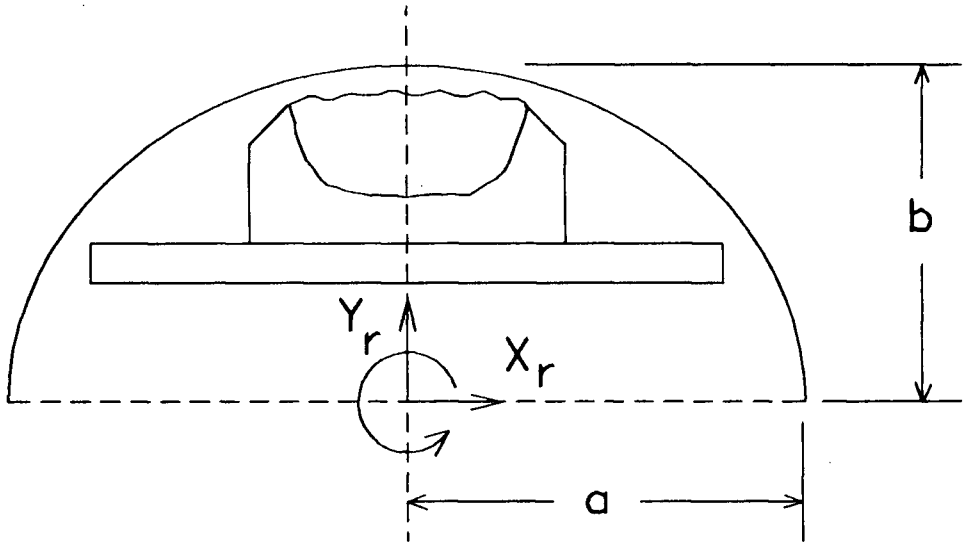

Figure 4.8: Encapsulating the table and cast with an ellipsoid

outline of the appliance. The order of application of the acrylic is performed back and forth across the rows of the grid, starting at the top left and proceeding left to right and then right to left on the next row. Once the machine has been placed over the first application point, movements to other application points can be made directly because of the small distances involved. Therefore, no collision avoidance is required once the machine has been placed over the first deposition point.

4.4.2 Collision Avoidance

After the inverse kinematic problem has been solved, a trajectory must be found that will move each of the axes to the desired position of acrylic application. The major considerations in choosing a path are collision avoidance and time of travel.

The collision avoidance problem is solved by representing the components of the machine as geometric entities and then calculating if the entities intersect as the machine moves. If they do, an alternate collision free path must be chosen. The rotary table and dental cast are encapsulated in an imaginary ellipsoid centred at the origin of the rotational stage and symmetric about the Z_t axis as shown in Figure 4.8. The pump, lamp and laser are the components most likely to collide with the rotary table and dental cast. The ends and edges of these components are represented by a series of points. By checking the relationship between these points and the ellipsoid, collision avoidance can be accomplished. Since the workspace of the acrylic pump and ultraviolet lamp is a plane, the problem can be reduced to a two-dimensional relationship between a series of points, representing the laser, pump and lamp, and an ellipse which is the cross-section of the ellipsoid through the workspace of the points. Therefore, the collision avoidance routine reduces to the problem of checking the intersection between an ellipse and a series of points.

To apply acrylic to a point on the dental cast when the initial position of the pump and lamp is outside the ellipse containing the dental cast and rotary table, the following method is used. First, the inverse kinematic problem is solved to find the required joint angles for acrylic application and curing at the desired position on the dental cast. The joint movements $\Delta\theta_r, \Delta\theta_t, \Delta L_3, \Delta L_5$ from the current position to the point of application are then calculated. The total number of point to point moves that will be used to accomplish the task, denoted N, is then calculated based on the distance ΔL_3 so that each move of the machine will result in a 2.54 mm movement of the horizontal linear axis. The position of the axes at each discrete point in the move is parameterized with respect to n as shown in (4.48) through (4.52).

$$\theta_r = \theta_{rstart} + n\Delta\theta_r/N \tag{4.48}$$

$$\theta_t = \theta_{tstart} + n\Delta\theta_t/N \tag{4.49}$$

$$L_3 = L_{3start} + n\Delta L_3/N \tag{4.50}$$

$$L_5 = L_{5start} + n\Delta L_5/N \tag{4.51}$$

$$n = 1, \ldots, N \tag{4.52}$$

At each of these parameterized locations, the points representing the pump, lamp and laser are checked to see if the proposed move would place them inside the ellipse. If so, the elevation L_5 is increased to place all the points outside or on the border of the ellipse.

In Figure 4.9, the ellipse surrounding the cast and table is shown with two coordinate frames, the machine base frame and the ellipse frame, and three points, P_1 through P_3. If the path generated using the parameterized equations was from ${}^bP_1$ to ${}^bP_2$, the path should be corrected to avoid collision. The collision free path would be from ${}^bP_1$ to ${}^bP_3$. In order to find the point ${}^bP_3$, the intersection points between the ellipse and the line $X_b = {}^bP_{2x}$ are found. The intersection points in base coordinates are found by first transforming the line into ellipse coordinates, finding the points of intersection between the line and the ellipse, and then transforming the points back to base coordinates. Then ${}^bP_{3y}$ is set to the larger Y value of the two intercepts.

Equations (4.53) and (4.54) give the equations for a line and an ellipse in the ellipse coordinate system. Equation 4.55 is the quadratic equation for the intersection between the line and the ellipse in terms of the X_e coordinate. This can be solved to find the X_e coordinates of the intersection between the desired path and the ellipse boundary. The

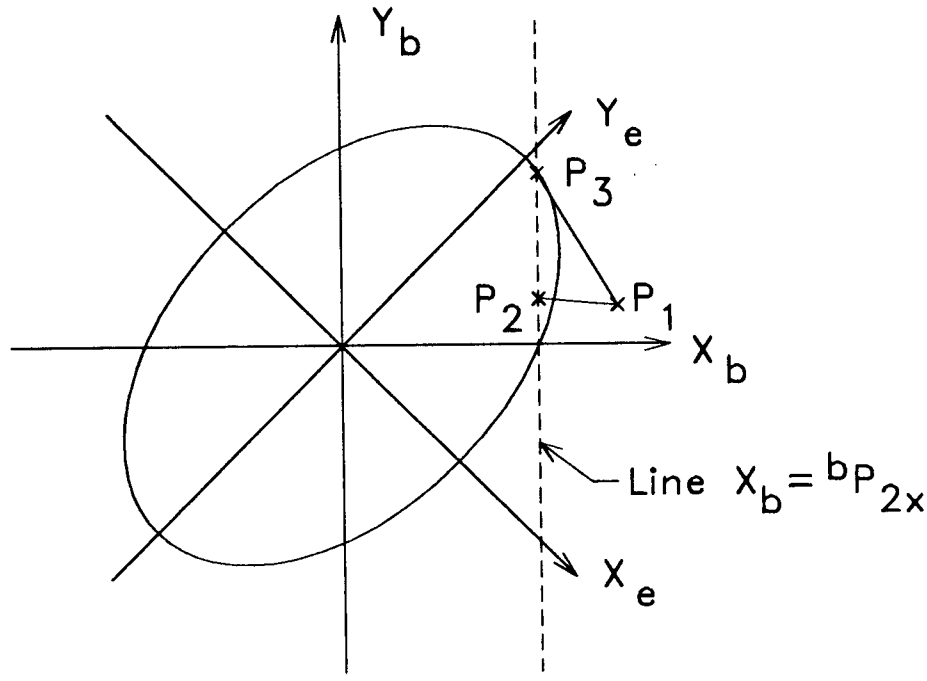

Figure 4.9: Collision avoidance

corresponding Y_e coordinates of the points of intersection are found by substituting the X_e values into (4.53).

$$y = y_1 + m(x - x_1) \tag{4.53}$$

$$\frac{x^2}{a^2} + \frac{y^2}{b^2} = 1 \tag{4.54}$$

$$(b^2 + a^2m^2)x^2 + 2a^2m(y_1 - mx_1)x + a^2(y_1^2 - 2x_1y_1m + x_1^2m^2 - b^2) \tag{4.55}$$

The above procedure is repeated for each parameterized location n on the path of motion. After the move when $n = N$, the pump nozzle will be on the ellipse directly above the point of application. The last move will be to bring the nozzle down to the desired elevation above the surface of the dental cast. Since the move distance between grid points has an upper bound of approximately 6 mm and the pump is offset approximately 5 mm from the surface of the dental cast, moves are made in a point to point fashion without collision avoidance calculations.

Chapter 5

Experimental Results

5.1 Machine Construction

A photograph of the orthodontic appliance manufacturing machine is shown in Figure 5.1. The machine was designed by the author and constructed in the U.B.C mechanical engineering machine shop.

5.2 Appliances

Many acrylic application and curing tests were performed, most of the tests involved applying and curing acrylic on the surface of a dental cast without any expansion screws or wires attached. Figure 5.2 shows a dental cast prepared for acrylic application. The wires and expansion screws are waxed to the surface of the cast with the correct clearance for acrylic application. Figure 5.3 shows the dental cast after the acrylic has been applied and cured by the machine.

Because of the poor reflective properties of the expansion screws, small caps are placed over the screws during scanning to provide a good reflection of the laser scan line. The acrylic flowed completely around the expansion screws and wires to provide good bonding in this appliance.

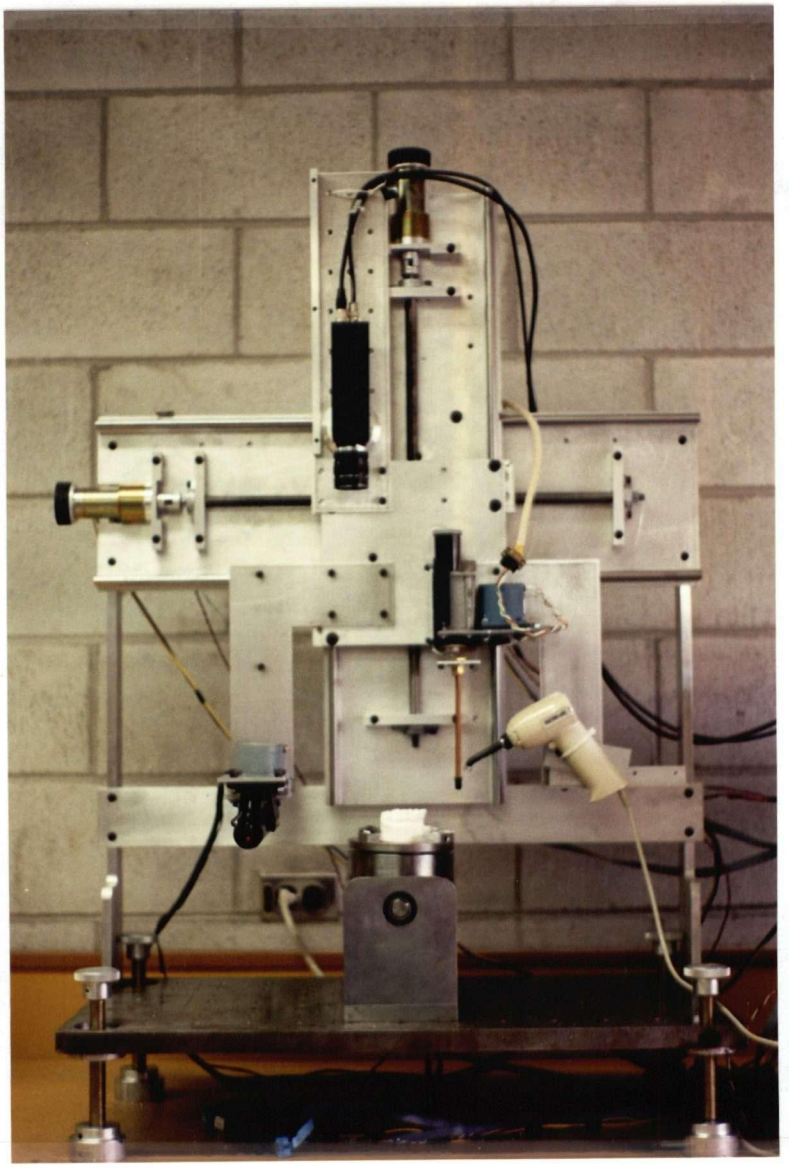

Figure 5.1: Experimental apparatus

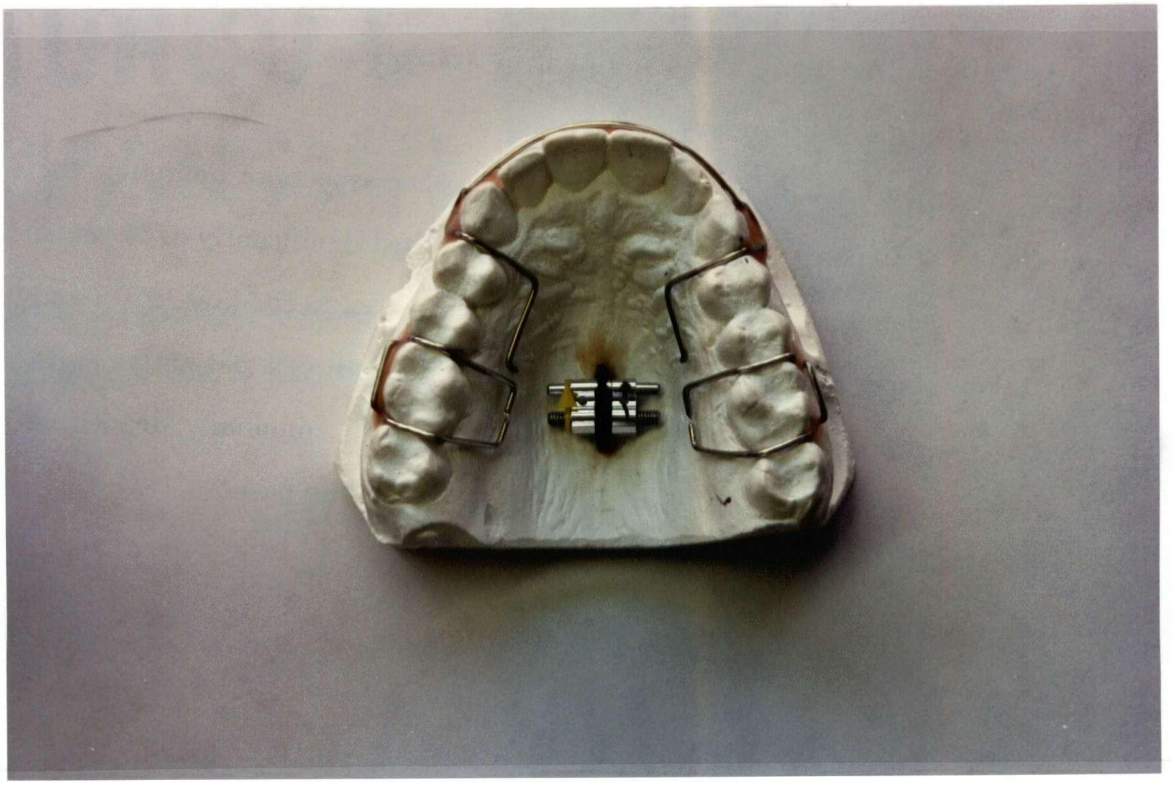

Figure 5.2: Dental cast with wires and expansion screw

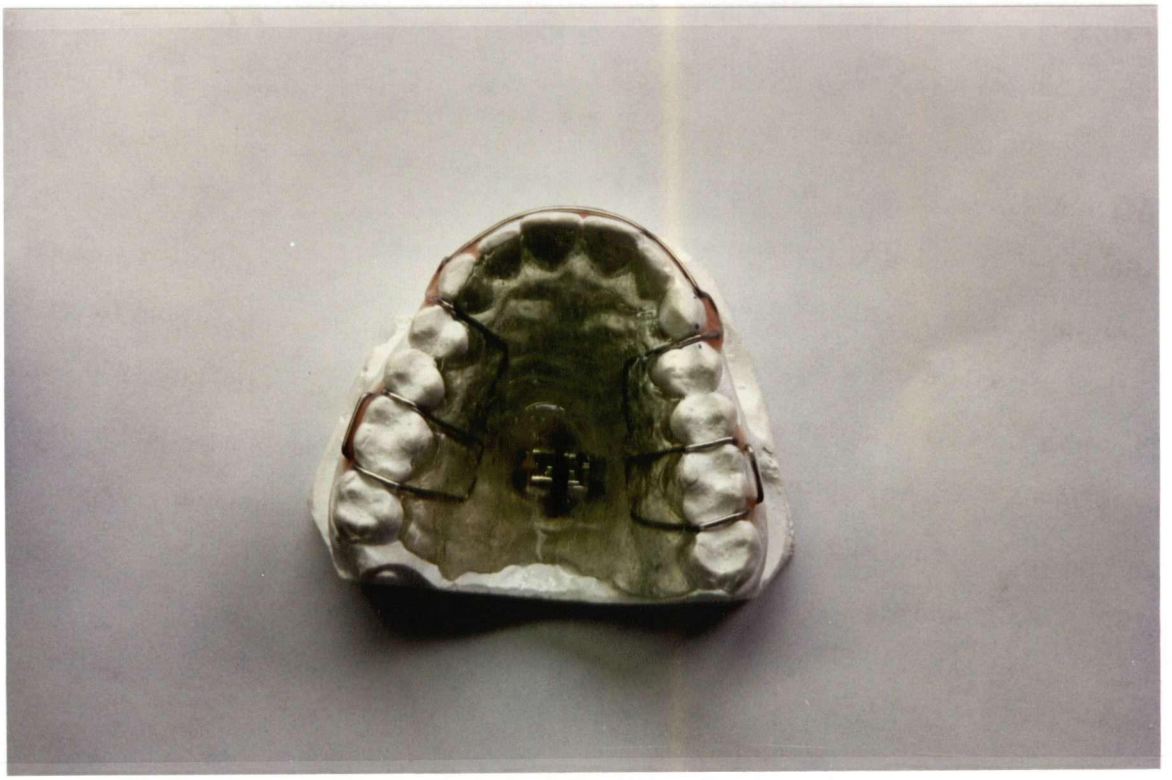

Figure 5.3: Finished appliance with wires and expansion screw

5.3 Acrylic Pump and Curing Lamp

In the current configuration, the pump and ultraviolet lamp are placed together to allow for acrylic deposition and curing without changing the machine position. However, a previous configuration was tried with the pump and lamp in different positions. In this first configuration, they were separated on the gantry by a horizontal distance of 109 *mm*. This allowed the pump and lamp to work independently over the surface of the dental cast without interfering with each other. The cast was oriented at the desired position for acrylic application, the pump was moved into position and acrylic was applied, then the lamp was positioned over the cast and the liquid acrylic was cured. However, as shown in Table A.3 of Appendix A, the number of separate acrylic application and curing cycles for the construction of one appliance ranges from 75 to 90. The added process time for these movements of the machine made this configuration unacceptable.

Currently, the pump and lamp are placed together so that the lamp shines on the area of acrylic deposition without movement of the machine. Using this configuration, it is necessary to have the lamp and pump placed so that both can perform their tasks without interfering with each other. This means that the pump cannot obstruct the lamp coverage of the surface. Also, neither the pump tip nor the lamp can be permitted to contact the surface. It has been difficult to find a combination of positions that satisfies these requirements. Longer curing times are required as the lamp is positioned further away from the surface than would be optimal. Tests with the lamp showed that it could pre-polymerize the acrylic in approximately 5 seconds from a distance of 1 *cm*. On the machine, however, the spacing between the acrylic and lamp during curing is approximately 2 *cm* and the corresponding pre-polymerization time is 15 seconds. Also, the pump nozzle still occasionally contacts the acrylic or dental cast during curing and the lamp occasionally contacts the cast during acrylic application. In order to avoid

these problems, two solutions have been considered. The first option is to construct a fibre-optic light conduit for the lamp that has a hole down the middle through which the acrylic could be pumped. This would mean that only one small tip would have to be positioned over the surface of the cast, avoiding the interaction of two pieces. The other option is to provide the lamp and pump with fast independent vertical motions using a solenoid. This would allow each component to move away from the area of deposition while the other is working.

During the tests, it was found that the ultraviolet lamp would overheat if it was run continuously. The times between the pumping and curing cycles are sufficient to keep the lamp from overheating during the pre-curing stage. However, for the final curing the acrylic must be radiated for 3 minutes, a length for which the current ultraviolet lamp is not suitable. Another lamp that covers the entire surface of the appliance and can be run continuously will have to be included in the system for any production prototype.

Acrylic flow rate was measured at 0.32 ml/min at room temperature with a time between drops of approximately 11 seconds. The pumping time was varied in order to change the thickness of the acrylic applied. The speed of the pump was not varied since at some speeds the stepper motor vibrated excessively and the flow rate dropped considerably. In order to accommodate for the 11 second period between acrylic drops from the pump nozzle, a patch size of approximately 4 $mm \times 4$ mm was used. This patch size also helped to decrease the total process time by reducing the total number of patches upon which material had to be applied.

Acrylic deposition and curing time tests for a range of appliances are shown in Table A.3 of Appendix A. The total lamp, pump and machine movement times are tabulated. The average time calculated from this data for the complete application and pre-curing process is 54.3 minutes. Of this time 16.6 minutes, 31% of the time, was spent pumping the acrylic and 20.75 minutes, 38% of the time, was spent pre-curing the

acrylic. By using a faster pump and placing the lamp closer to the area of curing, these times could be reduced considerably meaning much faster process times.

5.4 Image Processing

Several orientations of the cast and vertical increments of the laser plane were tested to determine the best combination for scanning the surface of the dental cast. The best orientations minimize the shadowing or occlusion of the surface of the dental cast from the laser light and camera positions. The final scanning technique involved four separate orientations of the cast. Data points were collected for the entire surface of the dental cast at each orientation. The vertical increment of the laser scan line during scanning was 0.76 mm. The orientations used are shown in Table A.2 in Appendix A.

Timing tests of the scanning process, summarized in Table A.2 of Appendix A show that the average scanning time for each cast is 11.5 minutes. This time could be improved by using a faster processor and further optimization of the image processing routines, perhaps writing more of the routines in assembly language.

The edge detection derivative operator, explained in Section 4.3.2, is used to detect the laser scan line on the surface of the dental cast. The operator used was $[1, 0, -1]$. Other operators such as $[2, 1, 0, -1, -2]$ and $[1, 1, 0, -1, -1]$ were also tried but did not give sufficiently better results to justify the extra computation involved.

5.5 Motion Control

The DC motors were controlled in constant velocity mode and in acceleration mode. The maximum speed used on the linear axes is 609.6 mm/min and the maximum rotational speed of the tables is 0.576 rad/sec. Homing the machine axes takes 135 seconds when the axes are at their centre positions to start.

5.6 Future Work

In Appendix B a comparison between the actual and in-plane surface normal was made for three dental casts. The results showed that most of the time the table was able to orient the cast within 25° of horizontal, the limit for flowing of the acrylic. However, for the casts tested, the percent of normals that fell outside this range was from 7.8 % to 17.0 %. For these sections of the dental casts the acrylic would most likely flow before it could be cured, resulting in an uneven surface. In order to avoid this uneven surface, two solutions have been considered. First, more degrees of freedom could be added to the machine resulting in better cast positioning. This is an expensive solution and should be a last resort. Secondly, the acrylic could be applied on the high side of the region in anticipation of running before cure. This solution seems viable since the surface contour data is available and the acrylic properties could be measured to predict material flow.

In order to produce a production model of this machine, the total process time must be reduced and an acrylic pump that provides a more even and faster flow must be used. A pump with a faster flow rate would decrease the process time and a more even flow rate would allow the use of smaller surface patches. A positive displacement piston pump could be used for this purpose.

Orthodontic labs usually make appliances out of two or more colours of acrylic. A pump that could switch between acrylic colours would be an advantage.

Independent motion between the pump and ultraviolet lamp would permit closer placement of the lamp to the acrylic, allowing faster curing times. This would also eliminate the problem of collisions between the pump, lamp and dental cast during the acrylic deposition process.

A method to improve the surface mapping and reduce the number of scans, would be to track which areas had been scanned and which areas needed scanning and adjust

the scanning method accordingly. Surface normal data from the regions already scanned could be used to orient the cast for scanning.

This thesis has concentrated on automating the deposition and curing of acrylic. However, automation of other parts of the process would add to the value of the machine. Partially formed wires could be developed to ease the appliance wire work and grinding and polishing tools could be added to the machine to perform the finishing work.

Chapter 6

Conclusions and Recommendations

The work described in this thesis has resulted in a system that partially automates the production of upper-mouth orthodontic appliances. The machine performs the deposition and curing required to manufacture the acrylic portion of the appliance. The mechanization of a process that until now has been performed by hand represents a contribution to the fields of robotics and manufacturing automation.

A custom designed, four axis computer-controlled robotic manipulator performs dental cast manipulation and surface mapping, as well as acrylic deposition and curing. A two-axis rotary table system provides the cast orientations required for mapping and acrylic deposition. The gantry positioned above the rotary table system allows access to the surface of the dental cast for the pump and ultraviolet lamp and provides motion for the camera and laser system. The path planning and collision avoidance software incorporated in the machine allow the system to operate autonomously.

A laser range finder maps the surface of the dental cast to obtain the elevation and surface normal data required by the process planning software. Range data accuracy is improved through the use of an algorithm that allows comparison and improvement of surface elevation data when the same point is mapped twice by the system. The surface elevation and surface normal data allow the machine to adapt the deposition and curing process plan for each new appliance.

Although the system has successfully produced orthodontic appliances, some improvements must be incorporated before the system can be used in a production environment.

The current process times for producing the appliance must be reduced by using a faster pump, providing independent motion of the pump nozzle and ultraviolet lamp, and speeding up the image processing software. A pump with a faster flow rate will significantly decrease the process time. By providing independent motion of the pump and ultraviolet lamp, the system will be able to bring the lamp closer to the cast surface resulting in lower pre-cure times. This will also eliminate any chance of contact by the lamp or pump nozzle with the surface of the dental cast during the deposition and curing process. Through refining the image processing software, the surface mapping times will be reduced.

Bibliography

[1] A.M. Biesada, *Tooth Tech: The New Dentistry*, High Technology Business, April 1989, pp. 28–31.

[2] R. Crawford, *Computers in Dentistry*, The Journal of the Canadian Dental Association, Vol. 54, No. 1, January 1988.

[3] K.F. Leinfelder, B.P. Isenberg, M.E. Essig, *A new method for generating ceramic restorations: a CAD-CAM system*, The Journal of the American Dental Association, Vol 118, June 1989.

[4] E.D. Rekow, D.R. Riley, A.G. Erdman and B.E. Klamecki, *CAD/CAM for Dental Restorations - Challenges and Possibilities*, IEEE Engineering in Medicine and Biology Society 11th Annual International Conference, 1989.

[5] K.L. Zakariasen, D.N. Dederich, J. Tulip, *Lasers in Dentistry*, The Journal of the Canadian Dental Association, Vol 54, No. 1, January 1988.

[6] T.M. Graber and B. Neumann, *Removable Orthodontic Appiances*, W.B. Saunders Company, 1984.

[7] C. Philip Adams, *The Design, Construction and Use of Removable Orthodontic Appliances*, 5th ed. Wright Publishing, 1984.

[8] K.D. Rudd, R.M. Morrow and J.E. Roads, *Dental Laboratory Procedures, Volume 3*, The C.V. Mosby Company, 1986.

[9] P.K. Allen, *Sensing and Describing 3-D Structure*, Proceedings of IEEE International Conference on Robotics and Automation, 1986, pp. 126–131.

[10] Arthur Browne and Leonard Norton-Wayne, *Vision and Information Processing for Automation*, Plenum Press, 1986.

[11] George G. Dodd and Lothar Rossol, eds. *Computer Vision and Sensor-Based Robots*, Plenum Press, 1979.

[12] R.C. Gonzalez and Paul Wintz, *Digital Image Processing*, Addison-Wesley Publishing Company, 1987.

[13] Berthold Horn, *Robot Vision*, MIT Press, 1986.

[14] Jorge L.C. Sanz, ed. *Advances in Machine Vision*, Springer-Verlag, 1988.

[15] Paul J. Besl,*Range Imaging Sensors*, Advances in Machine Vision, J. Sanz, Ed., Springer Verlag, 1989.

[16] J.P. Duncan, D.P. Dean, G.C. Pate, *Moiré contourography and computer aided replication of human anatomy*, Engineering in Medicine, vol. 9, no. 1, 1980, pp. 29–36.

[17] M. Samson, D. Poussart, D. Laurendeau, *3-D Range from Optical Absorbance - Application to Dental Imprint Measurements for Orthodontics Diagnosis*, IEEE Montech 87, 9–11 November, 1987, pp. 76–79.

[18] R.C. Bolles, P. Horaud and M.J. Hannah, *3DPO: A Three- Dimensional Part Orientation System*, International Journal of Robotics Research, vol. 5, No. 3 Fall 1986, pp. 3–26.

[19] C.H. Chen and A.C. Kak, *Modeling and Calibration of a Structured Light Scanner for 3-D Machine Vision*, IEEE International Conference on Robotics and Automation, 1987, pp. 807–815.

[20] S.W. Holland, L. Rossol and M.R. Ward, *Consight-1: A Vision-Controlled Robot System for Transferring Parts from Belt Conveyors*, Computer Vision and Sensor Based Robots, G. Dodd and L. Rossol ed., Plenum Press, 1979.

[21] S. M. Dunn and J. Yu,*Measuring the Surface Area of the Face*, IEEE Engineering in Medicine and Biology Society 11th Annual International Conference, 1989.

[22] X. Maldague, D. Poussart, D. Laurendeau and R. April, *Tridimensional Form Acquisition Apparatus*, SPIE Vol. 665 Optical Techniques for Industrial Inspection, 1986, pp. 200–208.

[23] J-L Jezouin, P. Saint-Marc, and G. Medioni, *Build an accurate range finder with off the shelf components*, Proceedings of International Conference on Computer Vision, June 5–9, 1988, pp. 195–200.

[24] M. Asada and S. Tsuji, *Shape From Projecting a Stripe Pattern*, Proceedings 1987 IEEE Conference on Robotics and Automation, pp. 787–792.

[25] K. Sugihara, K. Okazaki, F. Kaihua and N. Sugie, *Regular Pattern Projection for Surface Measurement*, Robotics Research, The Second International Symposium, Aug 20–23, 1894, pp. 17–24.

[26] Whoi-Yul Kim, *3-D Surface Reconstruction Using Cross- Stripe Structured-Light System*, Robotics and Manufacturing: Recent Trends in Research, Education and Applications, M. Jamshidi and M. Saif ed., Vol. 3, 1990, pp. 181–187.

[27] D. Poussart and D. Laurendeau,*3-D Sensing for Industrial Computer Vision*, Advances in Machine Vision, J. Sanz, Ed., Springer Verlag, 1989.

[28] Roger Y. Tsai, *An Efficient and Accurate Camera Calibration Technique for 3-D Machine Vision*, IEEE Proceedings of Conference on Computer Vision and Pattern Recognition, 1986, pp. 364–374.

[29] *Methyl Methacrylate Monomer Properties and Procedures for Handling and Use*, Dupont Plastics Department Bulletin, Wilmington, Delaware.

[30] Frank S. Stowe and Robert A. LieBerman, *Effect of Selected UV Bulbs and Photocatalysts On Multifunctional Acrylate Monomer/Homopolymer Properties*, Journal of Radiation Curing, V.12 (4), Oct 1985, pp. 16–18.

[31] Robert A. LieBerman, *Comparison of Several Trifunctional Acrylates Under Ultraviolet and Electron Beam Radiation Sources*, Journal of Radiation Curing, Vol. 11, No. 1, Jan 1984, pp. 22–29.

[32] *Occupational Health Guideline for Methyl Methacrylate*, U.S. Department of Labour, Occupational Safety and Health Administration, 1978.

[33] *Light-curing resins for plate-appliances and actuators*, Wil-O-Dont Light Cure System Users Manual, Wilde Dental, Germany.

[34] J. Craig, *Introduction to Robotics Mechanics and Control*, 2nd ed. Addison-Wesley Publishing Company, 1989.

[35] R. Paul, *Robot Manipulators*, MIT Press, 1981.

[36] J. Denavit and R.S. Hartenburg, *A Kinematic Notation for Lower-Pair Mechanisms based on Matrices*, Journal of Applied Mechanics, pp. 215–221, June 1955.

[37] Peter Lancaster, *Curve and Surface Fitting*, Academic Press, 1986.

Appendix A

Process Times

The surface scanning and acrylic deposition times were measured for four dental casts. The times are shown in the tables in this appendix. The length measurements are in millimeters and the times are in seconds unless otherwise specified.

Table A.1 lists the sizes of the four casts. These casts are representative of the size range of dental casts. The sizes shown are used by the system to optimize the resolution of the stored data and to control the scanning of the cast. The parameter C_{zmin} is the lowest elevation that will be scanned on the dental cast. C_{zmax} is the highest elevation that will be scanned on the dental cast. The width, C_{wid}, and length, C_{len}, of the dental cast are self-explanatory. C_{zb} is the height of the opening at the back of the dental cast.

Cast	C_{zmin}	C_{zmax}	C_{wid}	C_{len}	C_{zb}
A	3	25	69	51	8
B	5	28	61	53	8
C	8	28	71	61	15
D	15	36	76	61	20

Table A.1: Cast dimensions

Table A.2 lists the times for the surface elevation scanning and surface normal calculation for each cast. For each orientation given, sections were taken for elevations over the entire surface of the cast. The distance between vertical sections of the laser plane was 0.76 mm. The time for the surface normal calculation is also given. The elevation map for these scans was divided into a grid of 19×19 squares and surface normals were

calculated for each square. The total time for the scanning process is listed in the last row in seconds and in minutes.

Cast	A	B	C	D
$\theta_r = 10°, \theta_t = 0°$	132.3	145.34	118.0	129.4
$\theta_r = 40°, \theta_t = 0°$	213.7	230.6	229.4	237.1
$\theta_r = 30°, \theta_t = 30°$	145.0	158.6	138.4	149.0
$\theta_r = 30°, \theta_t = -30°$	143.0	156.7	137.7	148.4
Normal	39.8	40.3	34.2	34.2
Total [*min*]	673.7 [11.2]	731.6 [12.2]	657.7 [11.0]	697.9 [11.6]

Table A.2: Scanning times

Figure A.3 lists the acrylic deposition and pre-curing times for the dental casts. The lamp, pump and machine motion times are shown along with the total time. The number of patches that acrylic is deposited on is also shown.

Cast	*Lamp*	*Pump*	*Other*	*#Patches*	*Total* [*min*]
A	1305.0	1007.8	1030.2	87	3379.2 [56.3]
B	1125.0	701.25	944.4	75	2770.7 [46.2]
C	1200.0	1004.0	950.0	80	3154.9 [52.6]
D	1350.0	1271.7	1099.3	90	3721.0 [62.0]

Table A.3: Acrylic deposition and curing times

Figure A.4 shows the total surface scan, acrylic deposition and pre-curing and process times.

Cast	*Scan*	*Deposit*	*Total* [*min*]
A	673.7	3379.2	4052.9 [67.5]
B	731.6	2770.7	3502.3 [58.4]
C	657.7	3154.9	3812.6 [63.5]
D	697.9	3721.0	4418.9 [73.6]

Table A.4: Total process time

Figure A.5 shows the resolution of the data stored for each dental cast and the side length of the surface patches in millimeters.

Cast	*XY resolution* (S_{mxy})	*Z resolution* (S_{mz})	*Patch Size*
A	0.29	0.089	3.93
B	0.26	0.089	3.53
C	0.30	0.080	4.09
D	0.32	0.080	4.24

Table A.5: Resolution of stored data

Appendix B

Surface and In-Plane Normal Comparison

In Section 3.2 the claim was made that the two axis rotary table is sufficient to orient the dental cast for acrylic deposition. In order to avoid running, the cast must be oriented so that the surface of deposition is close to horizontal during the application and pre-curing of the acrylic. The angle between the actual and in-plane surface normal is the angle that the cast surface will be tilted from horizontal during acrylic deposition. This appendix presents data for the surface orientation during deposition for three dental casts. The surface elevation map for each cast was broken into a grid of 19×19 squares, the surface normal and in-plane normal was calculated for each square and the angle difference was calculated. A statistical analysis of the regions of a typical upon which acrylic is likely to be applied is presented below.

Tests with the acrylic material on the surface of the dental cast indicate that if the surface is within 25° of horizontal the material will not run significantly before curing takes place. Table B.1 shows the data obtained for three upper-mouth dental casts.

The experimental data indicates that the rotary table is able to orient the surface of

Sample	# Points	Ave	Min	Max	STD	# Above 25°	% Above 25°
A	135	13.26	0.07	45.5	10.91	23	17.0
B	141	9.16	0.22	38.6	8.86	11	7.8
C	121	11.29	0.77	36.5	8.44	10	8.2

Table B.1: In-plane normal orientation data

deposition within 25° most of the time. However, the percentage of points above 25° is as high as 17.0 % with a maximum angle of 45.5° for sample A. In these cases, material will flow before curing, resulting in uneven surface thickness on the appliance.

Appendix C

Image Processing Analysis

Table C.1 lists the values used for the image processing parameters. As described in Section 4.3.3, the category values are used to keep track of the laser scan line cross-sectional width. If a scan maps a point to a cell location that already contains elevation data, the category values are compared to determine whether the existing data will be replaced. Data from thinner scan sections is preferred.

Parameter	Description	Value
S_{edge}	Edge Detection Slope Threshold	25 $levels/pixel$
W_0	Width Category Value 0	12 $pixels$
W_1	Width Category Value 1	8 $pixels$
W_2	Width Category Value 2	4 $pixels$
S_c	Camera Calibration	0.1836 $mm/pixel$

Table C.1: Image processing parameters

Figure C.1 shows a typical distribution of cells mapped versus the width of the laser scan line. This shows that although the most common width is 2 pixels, widths of 6 pixels and higher are not uncommon.

Figure C.2 shows the number of cells for which the data mapped in Figure C.1 was replaced. This indicates that the data from the larger scan widths is being replaced as the scanning procedure maps the same point more than once.

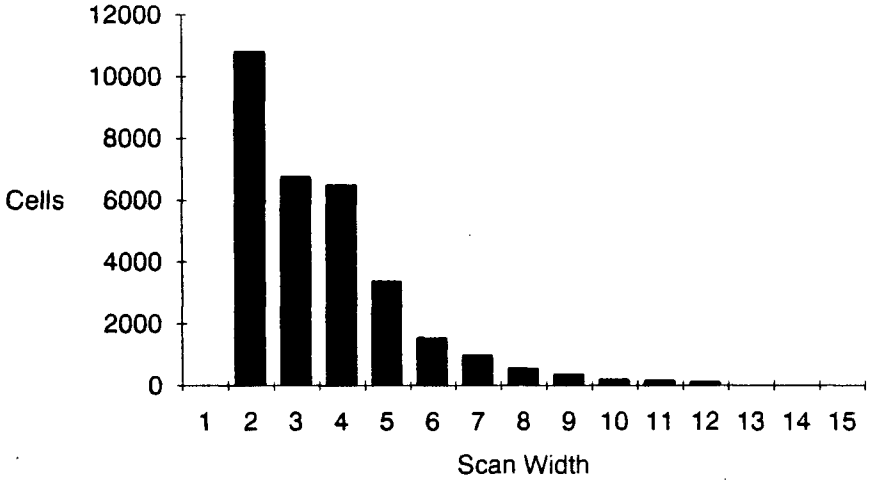

Figure C.1: Number of cells scanned versus scan width

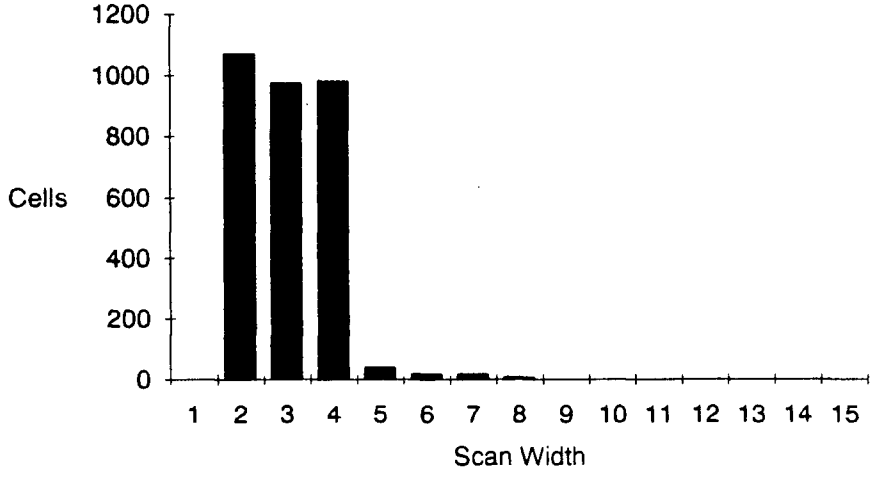

Figure C.2: Number of cells replaced versus scan width

Appendix D

Machine Kinematic Parameters

Table D.1 lists all the lengths used to calculate the machine kinematics. The lengths of constant parameters are listed in millimeters.

Parameter	Length mm
L_1	67.2
L_2	313.8
L_3	Horizontal gantry position
L_4	211.2
L_5	Vertical gantry position
L_6	120.7
L_7	180.3
θ_r	Rotational Stage Position
θ_t	Table Position

Table D.1: Machine parameters

Appendix E

Control Loop Parameters

The parameters for the D.C. motor control loop shown in Figure 3.6 in Section 3.2.5 are shown in Table E.1.

a	digital filter zero	-0.963
b	digital filter pole	0.500
K	digital filter gain	10.660
T	sample time	500 μS
K_I	amplifier gain	1.0 $amp/volt$
K_T	motor torque constant	29.2×10^{-3} Nm/Amp
J	armature inertia	1.54×10^{-6} $kg\ m^2$
K_e	encoder constant	636.6 rad^{-1}

Table E.1: Control loop parameters

Appendix F

Dental Cast Mapping Parameters

The parameters used in the mapping of the dental cast elevation data into the computer memory are listed in Table F.1.

Parameter	Definition	Value
C_{yoff}	CCD array offset from workspace	25 pixels
N_{grid}	Array size of grid squares	19 cells
N_{mxy}	Array size of range map	256 cells
N_{mz}	# of range map elevations	256 elevations
N_p	CCD array size	512 pixels

Table F.1: Dental cast mapping parameters

Appendix G

Process Flow Charts

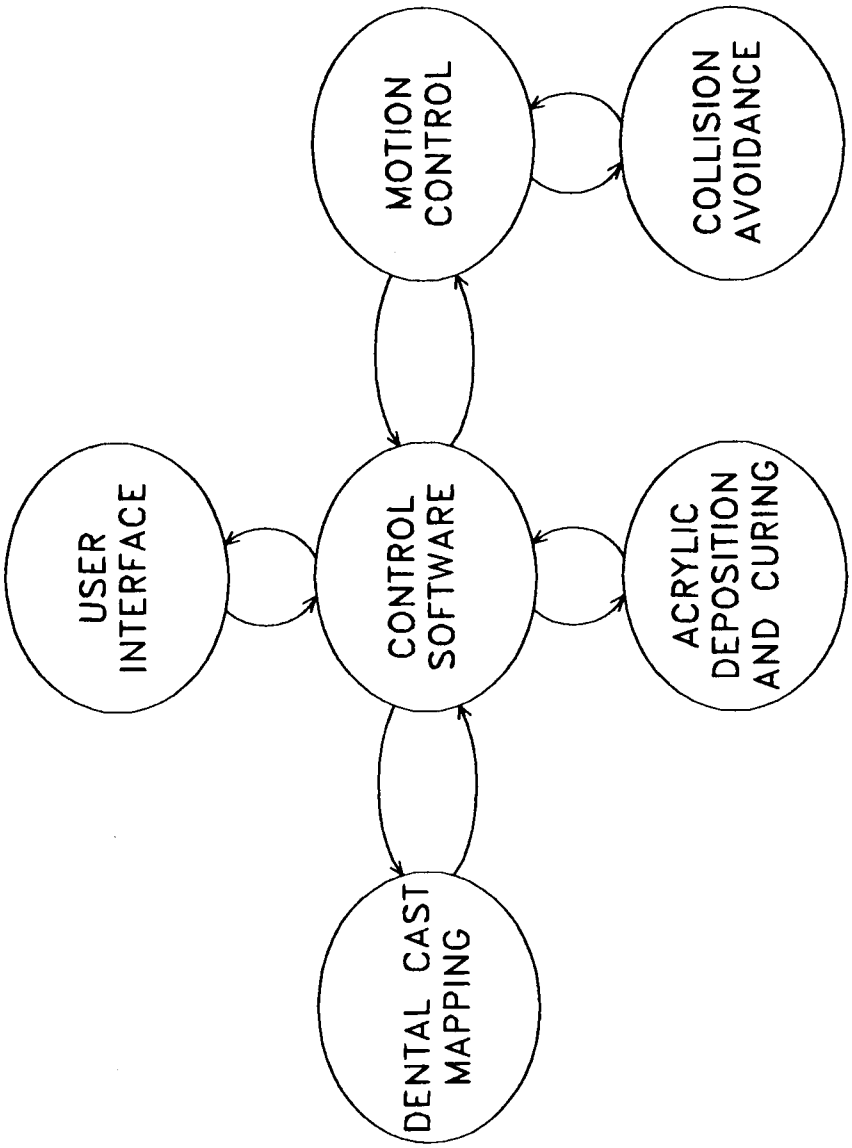

Figure G.1: Process overview flowchart

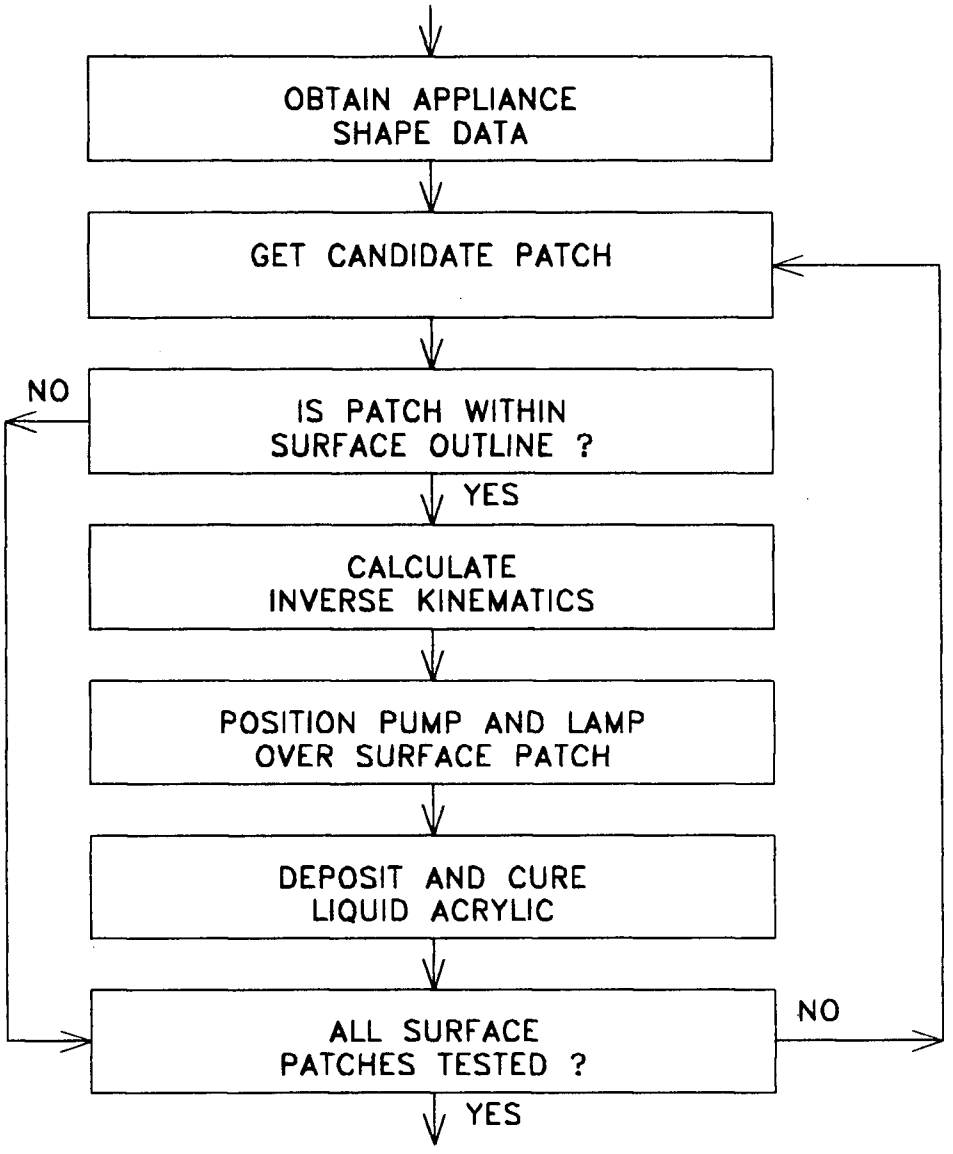

Figure G.2: Acrylic deposition and curing flowchart

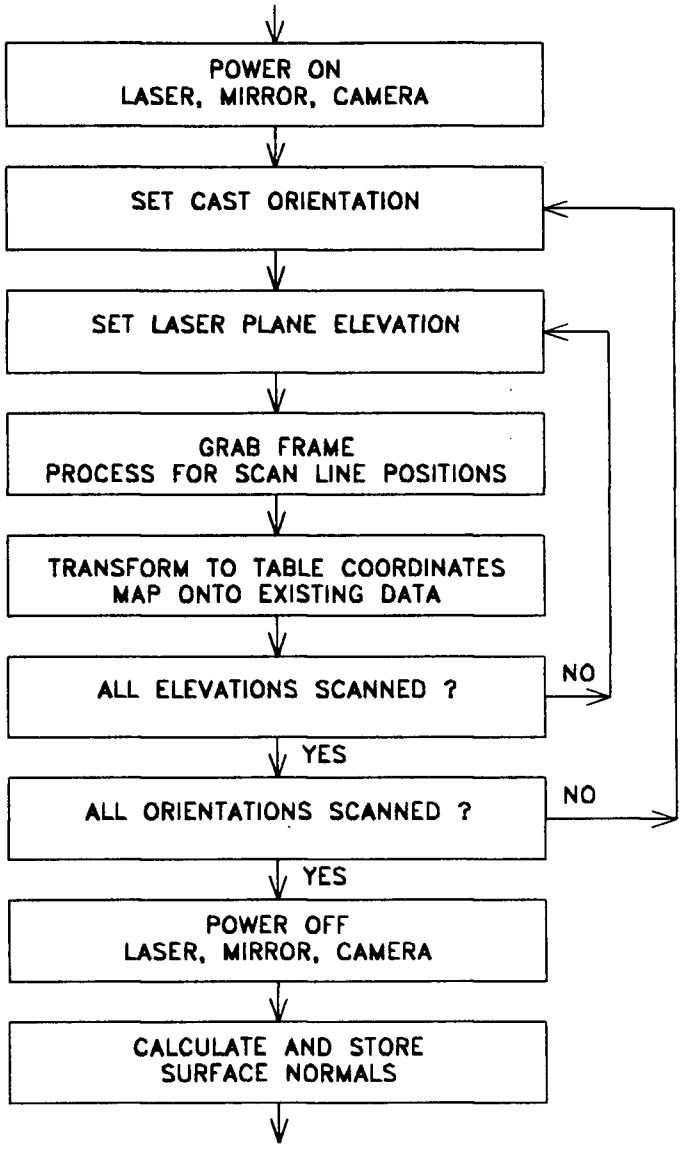

Figure G.3: Dental cast surface mapping flowchart